

DTIC FILE COPY

AD-A220 125



TIME-INTEGRATED SPECTRUM OF A
RADIATIVELY COOLING PLANCKIAN EMITTER

THESIS

Drew R. Fisher
Major, USAF

AFIT/GNE/ENP/90M-1

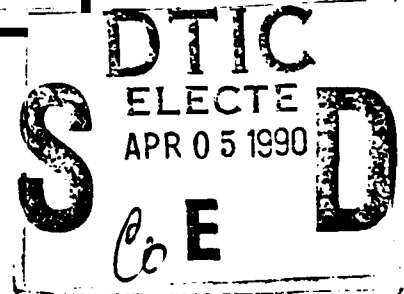
DISTRIBUTION STATEMENT A

Approved for public release;
Distribution Unlimited

DEPARTMENT OF THE AIR FORCE
AIR UNIVERSITY

AIR FORCE INSTITUTE OF TECHNOLOGY

Wright-Patterson Air Force Base, Ohio



90 04 05 114

AFIT/GNE/ENP/90M-1

TIME-INTEGRATED SPECTRUM OF A
RADIATIVELY COOLING PLANCKIAN EMITTER

THESIS

Drew R. Fisher
Major, USAF

AFIT/GNE/ENP/90M-1

Approved for public release; distribution unlimited

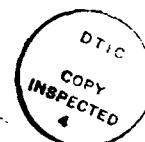
TIME-INTEGRATED SPECTRUM OF A RADIATIVELY COOLING
PLANCKIAN EMITTER

THESIS

Presented to the Faculty of the School of Engineering
of the Air Force Institute of Technology

Air University

In Partial Fulfillment of the Requirements for the Degree of
Master of Science



Drew R. Fisher, B.S.
Major, USAF

March 1990

Accession For	
NTIS	<input checked="checked" type="checkbox"/>
DTIC	<input checked="checked" type="checkbox"/>
Unprocessed	<input type="checkbox"/>
Justification	
By	
Distribution/	
Availability	
For	
A-1	

Acknowledgements

I owe many thanks to the Lord who provided support, love, and my sense of understanding; to my wife and children, Naomi, Dustin, and Andin, who supported me in this endeavor with love and patience through long, hard hours of work; and to my advisor LCDR Kirk A. Mathews, USN, for his gifted insight, his guidance, and also his patience.

Drew R. Fisher

Table of Contents

	Page
Acknowledgements	ii
List of Figures	v
Abstract	vii
I. Introduction	1
Background	1
Problem	3
Scope	3
Approach and Assumptions	4
Presentation	5
II. Theory	6
Definitions	6
Energy Balance	7
Concept of the Time-Integrated Spectrum	9
Change of Variables from Time to Temperature	10
Heat Capacity	12
III. Numerical Approximation	14
IV. Model 1 - Radiative Cooling with Constant, Material Heat Capacity, but No Radiation Heat Capacity	16
Model 1 Description	16
Heat Capacity	17
Planckian Spectra	18
Time-Integrated Spectra	20
Summary	24
V. Model 2 - Radiative Cooling with Temperature Consistent, Radiation Heat Capacity, but No Material Heat Capacity	26
Model 2 Description	26
Heat Capacity	27
Time-Integrated Spectra	28
Comparison with Planckian Spectra	32
Summary	33
VI. Model 3 - Radiative Cooling with Constant, Material Heat Capacity and Temperature Consistent, Radiation Heat Capacity	35

Model 3 Description	35
Heat Capacity	36
Time-Integrated Spectra	36
Comparison with Planckian Spectra	40
Summary	42
VII. Model 4 - Radiative Cooling with Temperature Consistent Heat Capacity	43
Model 4 Description	43
Binding Energy	44
Material Energy	50
Heat Capacity	51
Time-Integrated Spectra	52
Comparison with Planckian Spectra	56
Summary	59
VIII. Conclusions and Recommendations	60
Conclusions	60
Recommendations	61
Appendix A: Computer Program to Calculate the Time-Integrated Spectrum	62
Appendix B: Computer Program to Fit Time- Integrated Spectra with Two Planckian Basis Functions	74
Appendix C: Computer Programs to Calculate Binding Energy and Temperature	85
Bibliography	90
Vita	91

List of Figures

Figure	Page
1. Imploding Liner Pinch	2
2. Planckian Spectra a - d Normalized to Unit Area ...	19
3. Model 1 Time-Integrated Spectrum Normalized to Unit Area; $\theta_1=1$ KeV	20
4. Model 1 Time-Integrated Spectrum (Magnified View) Normalized to Unit Area; $\theta_1=1$ KeV	21
5. Model 1 Time-Integrated Spectrum Normalized to Unit Area; $\theta_1=10$ KeV	23
6. Model 1 Time-Integrated Spectrum Normalized to Unit Area; $\theta_1=0.02$ KeV	23
7. Planckian Spectra a - c Normalized to Unit Area and Multiplied by θ^3	29
8. Model 2 Time-Integrated Spectrum Normalized to Unit Area; $\theta_1=10$ KeV	30
9. Model 2 Time-Integrated Spectrum Normalized to Unit Area; $\theta_1=0.02$ KeV	31
10. Comparison of Time-Integrated Spectrum $\theta_1=1$ KeV with Planckian Spectra	31
11. Model 1, 2, and 3 Time-Integrated Spectra Normalized to Unit Area; $\theta_1=1$ KeV	38
12. Density Effect on Model 3 Time-Integrated Spectra Normalized to Unit Area; $\theta_1=0.02$ KeV	39
13. Density Effect on Model 3 Time-Integrated Spectra Normalized to Unit Area; $\theta_1=1$ KeV	40
14. Comparison of Two-Planckian Curve-Fit with Model 3 Spectrum; $N_v=1E+27$ particles/m ³	41
15. Comparison of Two-Planckian Curve-Fit with Model 3 Spectrum; $N_v=1E+29$ particles/m ³	41
16. Binding Energy versus Atomic Number Density for Carbon	47

17. Linear-Log Plot of Free Electrons per Atom versus Temperature for Copper	49
18. Smoothed Linear-Log Plot of Free Electrons per Atom versus Temperature for Copper	49
19. Linear-Log Plot of Binding Energy per Atom versus Temperature for Copper	50
20. Comparison of Model 4 Spectra Normalized to Unit Area; $\theta_1=1$ KeV, $N_v = 1E+27$ atoms/m ³	53
21. Linear-Log Plot of Change in Binding Energy per Atom with Respect to Temperature versus Temperature for Plutonium	55
22. Linear-Log Plot of Change in Free Electrons per Atom with Respect to Temperature versus Temperature for Plutonium	55
23. Comparison of Two-Planckian Curve-Fit with Model 4 Spectrum	56
24. Combination Curve-Fit for Model 4 Copper Spectrum	58
25. Comparison of Combination Curve-Fit with Model 4 Copper Spectrum	58

ABSTRACT

This paper investigates the effect of cooling a hot Planckian emitter upon its fluence spectrum . A sequence of models of increasing complexity is developed to determine the effects of various aspects of cooling upon the spectrum, such as initial temperature, density, and ionization state of the plasma. Spectra are calculated for radiating plasmas composed of different atomic number materials (carbon, aluminum, copper, and plutonium) at initial temperatures of 0.02 - 10 KeV, and initial densities of $1\text{E}+25$ - $1\text{E}+29$ atoms/m³, to observe the effects of these parameters on the fluence spectrum. The change in material and binding energy for some spectra at the low energy end produces a second, prominent but smaller peak. The resulting non-Planckian spectra can be approximated with two or more Planckian basis functions having different temperatures.

TIME-INTEGRATED SPECTRUM OF A RADIATIVELY COOLING PLANCKIAN EMITTER

I. Introduction

This paper deals with computing the spectral distribution of thermal radiation emanating from an extremely hot body, and how cooling effects its spectrum taken over time.

Background

Astronomers have long been interested in the spectral character of radiation coming from hot bodies such as stars, quasars, and supernovas, to obtain clues to their makeup, temperature, age, and internal processes that occur in their life cycle. It is generally recognized that nuclear fusion is the process that heats the cores of stars to extremely high temperatures (millions of degrees Kelvin), and causes them to radiate enormous quantities of energy.

Currently, there is much research effort going on worldwide to achieve a controlled and sustained source of fusion energy as an alternative to other sources of energy. Fusion experiments, then, can serve as likely sources for studying the spectral nature of hot bodies (plasmas) undergoing spontaneous cooling, once the power source is shut off.

One example of an experimental setup that is capable of achieving high temperatures in a plasma (although not yet to the point of fusion ignition) is the imploding liner pinch illustrated in Figure 1, adapted from (1:315).

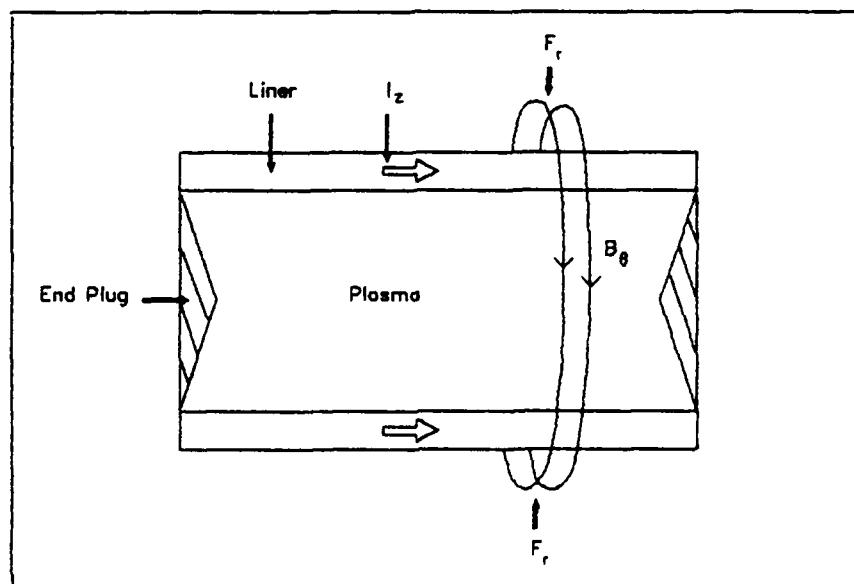


Fig. 1. Imploding Liner Pinch

A plasma is contained within a cylindrical thin metal tube or liner through which a large electric current, I_z , is passed. The axial-directed current induces an azimuthal magnetic field, B_θ , around the liner. Both current and magnetic field interact together to produce a radial, inward-directed force, F_r , that causes the liner and plasma to implode. The compressive force and inertial momentum of the liner are eventually halted by the increasing plasma pressure from within, but by that time compres-

sion has superheated both plasma and liner past the point of vaporizing and ionizing the liner material which becomes a part of the plasma.

In order to predict the spectral behavior of a hot body, such as the plasma in the imploding liner pinch, through a mathematical model, it is sometimes assumed that the temperature of material and radiation is the same, therefore the distribution of radiant energy emitted from the body's surface can be described as Planckian. This study also assumes this. However, integrating the spectrum over time, i.e., the time-integrated spectrum or fluence spectrum, should show the behavior to be non-Planckian.

Problem

The purpose of this study is to investigate the effects of cooling on the fluence spectrum of a Planckian emitter. In addition, the spectrum is compared to a Planckian curve-fit spectrum to determine the validity of approximating the fluence spectrum with Planckian basis functions.

Scope

The study is computational and analytic rather than experimental, so the results are predictive in nature. Three parameters are varied as initial conditions for the Planckian emitter to observe their effects during cooling. These are temperature, density, and material composition. The initial temperature range is 0.02 - 10 KeV, and the

emitter is allowed to cool to about $1/50,000$ th of the initial temperature. Densities range from $1E+25$ - $1E+29$ atoms per cubic meter, and material composition is one of the following elements: carbon, aluminum, copper, or plutonium.

Approach and Assumptions

A sequence of models is considered that increases in complexity according to the type of internal energy assumed to be contained within the emitter, whether it be material energy, radiation energy, or a combination of both, etc.

These models and their assumptions are as follows:

Model 1 - Radiative Cooling with Constant, Material Heat Capacity, but No Radiation Heat Capacity.

- The volume is constant; this model excludes cooling by expansion.
- Local thermodynamic equilibrium exists between matter and radiation.
- The temperature is uniform throughout the volume at any instant, but varies with time.
- The heat capacity remains constant throughout the cooling process.

Model 2 - Radiative Cooling with Temperature Consistent, Radiation Heat Capacity, but No Material Heat Capacity.

- The above assumptions apply except the radiation heat capacity varies with temperature.

Model 3 - Radiative Cooling with Constant, Material Heat Capacity and Temperature Consistent, Radiation Heat Capacity.

- The assumptions of Model 1 and 2 taken together apply to this model, with clarification that the heat capacity contributed by material is constant, and the heat capacity contributed by radiation changes with temperature.

Model 4 - Radiative Cooling with Temperature Consistent Heat Capacity.

- Model 3 assumptions are retained except:
- The material heat capacity is allowed to vary according to the ionization state of the atoms which is dependent on temperature.

Presentation

Chapter II presents the general analytic form and theory behind calculating the time-integrated spectrum, and Chapter III shows the numerical approximation for the analytic form. Then Chapters IV - VII present the models in order as discussed above along with results and discussion of the computed spectra. Conclusions and recommendations are included in Chapter VIII.

II. Theory

Let us start with a definition of the radiatively cooling Planckian emitter and its surroundings, followed by some assumptions about how they interact through the law of energy conservation, then develop the concept of a time-integrated spectrum, first as a function of time, then as a function of temperature. From the latter development, it becomes apparent that heat capacity plays a major role in the spectrum behavior.

Definitions

The initially hot body under consideration can be any collection of ions, electrons, and neutral atoms from a single element constrained to an arbitrary, constant, finite volume. For initial temperatures of 0.02 to 10 KeV undertaken in this study ($1 \text{ KeV} = 11,600,000 \text{ K}$) and densities of $1\text{E}+25$ to $1\text{E}+29$ particles/ m^3 , an optically thick plasma is an appropriate description for the hot body. Within the volume, the material particles collide with one another giving rise to radiation particles or photons which in turn are absorbed or scattered by the material particles. At any given time, a fraction of these photons reach the volume boundary and radiate outward, away from the body, depleting the plasma of its internal energy. The loss of energy is equivalent to lowering the temperature of the plasma, hence it cools by radiative emission.

Besides the process of radiative cooling, two other mechanisms exist for cooling the body. They are the transfer of kinetic energy from material particles to the wall or force field defining the volume boundary, and expansion of the volume; however, neither cooling mechanism is considered in this study.

At any instant in time, assuming the radiation temperature is the same as the kinetic temperature of the material particles in a condition of local thermodynamic equilibrium, the photon energy distribution can be described by the Planck function at some average temperature. Thus, the cooling emitter is Planckian in nature.

Just beyond the plasma boundary lies an infinite, empty universe at temperature $T=0$ Kelvin into which the radiation escapes. It is assumed that there is no flux of radiation into the volume.

Energy Balance

Having defined the cooling emitter and its surroundings, let us now account for the gain and loss in energy of the plasma through a differential energy balance equation. In general, the change in total internal energy of the plasma with respect to time is equal to the heat flux in minus the heat flux out of the plasma, plus heat coming from any internal source minus heat lost to any internal sink, minus work done by the expanding material. This is expressed in the equation:

$$dU/dt = \dot{Q}_{\text{flux in}} - \dot{Q}_{\text{flux out}} + \dot{Q}_{\text{source}} - \dot{Q}_{\text{sink}} - \dot{W}_{\text{by}} \quad (1)$$

where the dot over a variable denotes differentiation with respect to time. Since there is no flux of radiation into the body from the outside universe, the term for heat flux in is zero. Regarding the source term, the supply of energy to heat the plasma has stopped (by assumption) so this term is also zero. The heat sink term represents energy absorbed by the material particles in endothermic reactions, but it is assumed that the particles do not react, therefore this term vanishes. One more term vanishes because the volume remains constant with time: the work term, which can be defined as pressure times the change in volume with respect to time.

Now the change in internal energy per unit time is that which radiates out through the surface area in the same amount of time:

$$dU/dt = -\dot{Q}_{\text{flux out}} = -\sigma T_s^4 A \quad (2)$$

where σT_s^4 is the energy per unit area emitted per unit time from the total surface area A ; T_s is the surface temperature; and σ is the Stefan-Boltzmann constant. In the above equation the minus sign signifies a loss of energy to the surrounding universe. The term σT_s^4 is a result of Stefan's law for black body radiation (2:4), and is equivalent to the Planck distribution of energy per unit area per unit time $\rho_\lambda(E, T_s)$ integrated over all photon energies $E = h\nu$ (h is

Planck's constant and ν is frequency) at temperature T_s . This surface temperature is the same as the average internal temperature at time t , and is hereby designated $T(t)$.

Concept of the Time-Integrated Spectrum

Let

$$p_A(E, t) = p_A(E, T(t)) = p_A(E, T_s) \quad (3)$$

be the Planck function that describes the energy distribution per unit area per unit time so that

$$\int_0^\infty p_A(E, t) A dE = \sigma [T(t)]^4 A \quad (4)$$

If the hot body starts with initial internal energy U_i and is allowed to cool forever, it will eventually lose all its energy such that the following expression holds true:

$$U_i = \int_0^\infty \sigma [T(t)]^4 A dt \quad (5)$$

hence

$$F = \int_0^\infty \int_0^\infty p_A(E, t) A dE dt = U_i \quad (6)$$

and defining

$$f(E) = \int_0^\infty p_A(E, t) A dt \quad (7)$$

equation (7) is the distribution function that describes the time-integrated spectrum, which upon normalizing to unit area is given by

$$g(E) = \frac{f(E)}{F} \quad (8)$$

Change of Variables from Time to Temperature

So far, the development of the time-integrated spectrum has dealt explicitly with the time behavior of the radiation energy distribution, with temperature being a function of time. This requires knowledge of how the temperature varies with time, which may not be well known. An equivalent and easier approach is to determine the behavior as a function of temperature so that the integration of equation (7) is performed over temperature instead of time. This approach eliminates the need to know the time behavior explicitly, and the end result is the same: the fluence spectrum (or time-integrated spectrum).

Referring back to equation (7), the integration variable is changed from time to temperature:

$$f(E) = \int_{T_i}^{T_f} p_A(E, T) A \frac{dt}{dT} dT \quad (9)$$

where the initial temperature T_i corresponds to $t_i=0$, and the final temperature T_f corresponds to $t_f=\infty$ which may be considered as $T_f=0$, and

$$p_A(E, T) A = \frac{2\pi}{c^2 h^3} \left[\frac{E^3}{e^{(E/kT)} - 1} \right] A \quad (10)$$

is the Planck distribution of energy per unit time. Equation (10) is adapted from (2:24) in terms of energy instead of frequency. h is Planck's constant, c is the speed of light in a vacuum, and k is Boltzmann's constant.

Before proceeding further, dt/dT in equation (9) can be transformed by considering the change in total internal energy as a total derivative with respect to time, volume, and temperature in which the concept of heat capacity is introduced:

$$\frac{dU}{dt} = \frac{\partial U}{\partial t} \left(\frac{dt}{dt} \right) + \frac{\partial U}{\partial V} \left(\frac{dV}{dt} \right) + \frac{\partial U}{\partial T} \left(\frac{dT}{dt} \right) \quad (11)$$

In the first term on the right hand side, $\partial U/\partial t$ is zero because the internal energy does not change with just the passage of time and no other influences. In the second term, there is no change in volume V as stated before, so this term is zero. Only the third term remains which contains within it the definition of heat capacity, that is

$$C(T) = \text{heat capacity} = \partial U / \partial T \quad (12)$$

which is the change in energy per unit change in temperature. Combining equations (2), (11), and (12) and rearranging terms results in the desired transformation for dt/dT :

$$dt/dT = -C(T)/\sigma T^4 A \quad (13)$$

Now equation (9) becomes

$$f(E) = - \int_{T_1}^{\infty} \frac{C(T) p_A(E, T) A}{\sigma T^4 A} dT \quad (14)$$

Let $p_A(E, T)A$ be normalized to unit area in the following manner with T as a parameter:

$$\rho(E;T) = \frac{p_A(E,T)}{\sigma T^4} \frac{A}{A} \quad (15)$$

$$= \frac{2\pi}{c^2 h^3 (\sigma T^4)} \left[\frac{E^3}{e^{(E/kT)} - 1} \right] \quad (16)$$

$$\sigma = \frac{2\pi^5 k^4}{15 c^2 h^3} \quad (2:24) \quad (17)$$

$$\rho(E;T) = \frac{15}{(\pi k T)^4} \left[\frac{E^3}{e^{(E/kT)} - 1} \right] \quad (18)$$

$$\int_0^\infty \rho(E;T) dE = 1 \quad (19)$$

Incorporating $\rho(E;T)$ into equation (14) and interchanging the order of integration yields:

$$f(E) = \int_0^{T_1} \rho(E;T) C(T) dT \quad (20)$$

This expression says that the time-integrated spectrum at photon energy E has a value equal to the sum of the released energy with a certain distribution at each temperature T from the initial temperature down to zero. By integrating equation (20) over all energy E and dividing the result into equation (20), the result is the normalized fluence spectrum equivalent to equation (8) at any energy E :

$$S(E) = \frac{f(E)}{\int_0^\infty f(E) dE} = \frac{f(E)}{F} \quad (21)$$

Heat Capacity

Up to this point, we have explicitly defined the normalized Planck function $\rho(E;T)$ in equation (18), but have not explicitly defined the heat capacity $C(T)$ needed to

calculate the time-integrated spectrum. Since heat capacity is the change in internal energy with respect to temperature, a question to ask is how the internal energy of the plasma varies with temperature. A general formula for the total internal energy U as a function of temperature is:

$$U(T) = U_m(T) + U_r(T) + U_{lh}(T) \quad (22)$$

where U_m is the material energy; U_r is the internal radiation energy; and U_{lh} is the energy due to latent heats of transformation. U_{lh} is comprised of several terms that describe the energy required to change the material state: that from solid to liquid (latent heat of fusion), from liquid to vapor (latent heat of vaporization), and once in the vapor state, to ionize or strip off electrons from the atoms (latent heat of ionization). Specific forms of $C(T)$ are deferred to the corresponding chapters that talk about how each term in equation (22) affects the fluence spectrum through $C(T)$.

III. Numerical Approximation

Equations (20) and (21) , representing the non-normalized and normalized fluence spectrum, respectively, are difficult to solve analytically. Therefore, numerical methods are employed with the use of a computer to approximate the solutions to these equations.

For convenience, temperature is redefined as $\theta = kT$, having units of energy. Both θ and E are expressed in KeV throughout the remainder of the paper.

Simpson's rule of integration is used for both integration over temperature and energy, with the limits of integration altered slightly from the original limits. For the lower limits, θ and E cannot assume the value of zero because either condition causes division by zero in equations (20) and (21). Therefore, the lowest value for θ is a final temperature of $\theta_f > 0$, and that for E is $E_{low} > 0$. An upper limit of $E = \infty$ is likewise impossible to evaluate numerically in a computer solution, thus $E_{high} < \infty$. In fact, E_{high} does not need to be more than about $30\theta_f$ because the upper tail of the spectrum (plot of $f(E)$ or $g(E)$ versus E) always decreases monotonically to zero by $E = \infty$, for all forms of $C(\theta)$ considered in this study, and the area under the tail in this region is negligible compared to the area beneath the spectrum curve at energies less than $30\theta_f$.

Another problem arises with how large a number the computer can handle. In particular, a program execution error occurs if the ratio E/θ in the exponential term in the denominator of $\phi(E;\theta)$ is too large (approximately 709 encountered in this study). This condition occurs at all energies when $\theta \ll E$. Again, for the forms of $C(\theta)$ presented in this study, and at any fixed E in the range $0 < E < 30\theta_1$, the integrand of equation (20) adds a negligible contribution to $f(E)$ at temperatures below about $\theta = E/50$.

Taking into account the above observations, the numerical approximation for equation (20) is:

$$f(E) \approx \int_{\theta_1}^{\theta_2} \phi(E;\theta) C(\theta) d\theta, \quad \theta_1 = E/50 > 0 \quad (23)$$

Note that the lower temperature limit changes with E . The approximation for equation (21) is:

$$\bar{g}(E) = \frac{f(E)}{F} \approx \frac{f(E)}{\int_{E_{\text{high}}}^{E_{\text{low}}} f(E) dE}, \quad E_{\text{low}} > 0, \quad E_{\text{high}} = 30\theta_1 < \infty \quad (24)$$

For the above two equations,

$$\phi(E;\theta) = \frac{15}{\pi^4 \theta^4} \left[\frac{E^3}{e^{E/\theta} - 1} \right] \quad (25)$$

and $\bar{C}(\theta) = dU/d\theta$ take on the specific forms addressed in the next several chapters.

IV. Model 1 - Radiative Cooling with Constant, Material Heat Capacity, but No Radiation Heat Capacity

In this chapter, we look at a description of the model; develop a specific form of heat capacity to be used in equation (23); predict the time-integrated spectrum behavior with a collection of one-temperature Planckians; and present and discuss the results of calculating the time-integrated spectrum for three different initial temperatures.

Model 1 Description

The first model deals only with the material particles losing kinetic energy. That kinetic energy is converted to radiation energy which radiates into space from the surface of the plasma volume. It does so at a rate that corresponds to the release of an equal amount of energy for every degree drop in temperature. In other words, the material heat capacity is constant; it is independent of temperature. The internal radiation density, on the other hand, must be negligible compared to the material energy density to assume there is little or no radiation heat capacity, that is to say, very little loss of internal radiation energy per degree change in temperature. In the absence of internal radiation energy ($U_r(\theta) \sim 0$) and internal energy to ionize to any degree most of the atoms ($U_{be}(\theta) = U_{lu}(\theta) \sim 0$, where "be" stands for binding energy), this model, in general, represents cooling behavior at temperatures much lower than about

0.001 KeV (on the order of 100,000 K), the temperature at which $U_r(\theta)$ and $U_{ee}(\theta)$ become significant compared to the material energy, $U_m(\theta)$. This will become evident in chapters VI and VII where $U_r(\theta)$ and $U_{ee}(\theta)$ are discussed relative to $U_m(\theta)$, respectively. However, the model is extended to higher temperatures to observe the cooling behavior of this limiting case. This simple model is used to demonstrate the methodology and, as a limiting case, to show how very non-Planckian the fluence spectrum can be.

Heat Capacity

The expression for $C(\theta)$, or actually just C since the heat capacity in this case is independent of temperature, is derived from the expression for the material energy only, $U_m(\theta)$ in equation (22). Assuming the material particles exhibit a Maxwell-Boltzmann distribution in energy, the average kinetic energy of any particle is $(3/2)kT = (3/2)\theta$ (3:12). Multiplying this by the total number of particles, and dividing by the volume gives the material energy density:

$$u_m(\theta) = U_m(\theta)/V = N_v(3/2)\theta \quad (26)$$

where u_m is the material energy density; and N_v is the atomic number density. Taking the derivative with respect to temperature gives the heat capacity per unit volume:

$$C_v = C/V = du_m/d\theta = N_v(3/2) \quad (27)$$

which is constant, provided the number density remains constant throughout the cooling process. (Ionization is disregarded until Model 4). Replacing C_v for $C(\theta)$ in equation (23), it is possible to bring C_v outside the integral sign as a constant so that equation (24) becomes:

$$\dot{S}(E) \approx \frac{C_v \int_{\theta_f}^{\theta_i} \dot{p}(E; \theta) d\theta}{C_v \int_{E_{low}}^{E_{high}} \int_{\theta_f}^{\theta_i} \dot{p}(E; \theta) d\theta dE} \quad (28)$$

Because C_v cancels in the above equation, it can assume any constant value without loss of generality. Therefore, $C_v = 1$ to simplify calculation of equation (28).

Planckian Spectra

Note that with $C_v = 1$, the numerator of equation (28) becomes a sum of normalized Planckians at different temperatures over the full range of E . Figure 2 displays several normalized Planckian spectra at various temperatures calculated from equation (25). This figure serves to show the expected trend for the curve of the fluence spectrum. Curve e, which is not normalized, is the sum of curves a through d, and represents the approximate shape of the fluence spectrum. It shows that as the temperature continues to drop, a greater percentage of the total energy is carried away by lower energy photons or, equivalently, lower frequency photons.

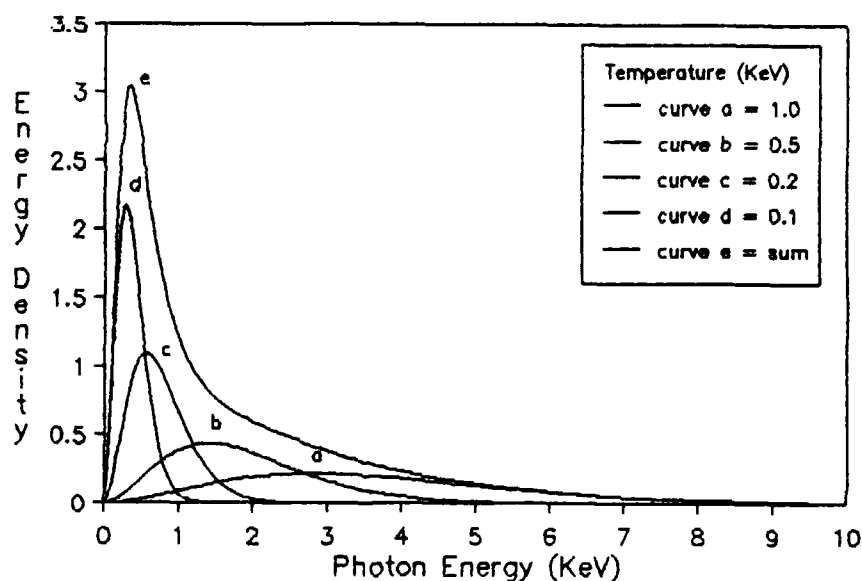


Fig. 2. Planckian Spectra a - d
Normalized to Unit Area

Mathematically speaking, the curve should continue to infinity by $\bar{E}=0$ for the following reason. If $\bar{E}=\theta$ in equation (25), then the portion of the equation equal to $15/(\pi^4 \exp(\bar{E}/\theta) - 1)$ remains constant, even as both \bar{E} and θ approach zero. However, θ^4 in the denominator becomes the dominant factor causing \bar{D} to approach infinity as it approaches zero. For any fixed θ greater than zero, and as \bar{E} approaches zero, the \bar{E}^3 term in the numerator decreases faster than the denominator, and is the reason why all of the above spectra diminish to zero by $\bar{E}=0$. Adding more Planckians to Figure 2 would enlarge curve e, but the curve should retain its approximate shape. Lower temperature Planckians added successively to the left of curve d would add diminishing areas to the total area underneath curve e.

Thus, when curve e is normalized to unit area, the peak should reach some finite limit at the left edge of the graph.

Time-Integrated Spectra

Time-integrated spectra with initial temperatures of 0.02, 1, and 10 KeV are calculated from equation (28) using the computer program listed in Appendix A.

Figure 3 shows the time-integrated spectrum with an initial temperature of 1 KeV.

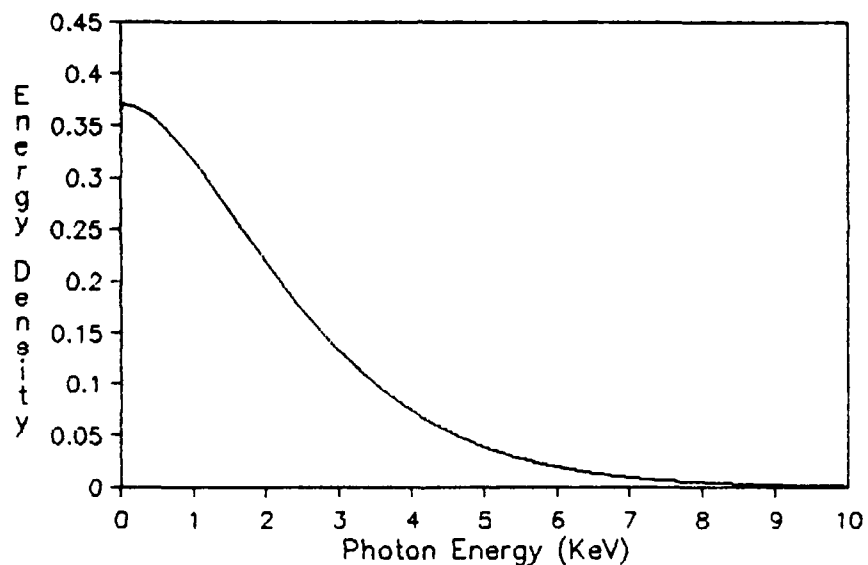


Fig. 3. Model 1 Time-Integrated Spectrum
Normalized to Unit Area; $\theta_i = 1$ KeV

Indeed, the spectrum curve has roughly the same shape as curve e in Figure 2 from the peak to the upper end of the spectrum, and the peak approaches a limiting value of about

0.37 relative units of energy density. Upon closer examination at the left edge of the graph shown in Figure 4, the spectrum curve rolls over at about $E=0.01$ to drop to just less than 0.05 near $E=0$.

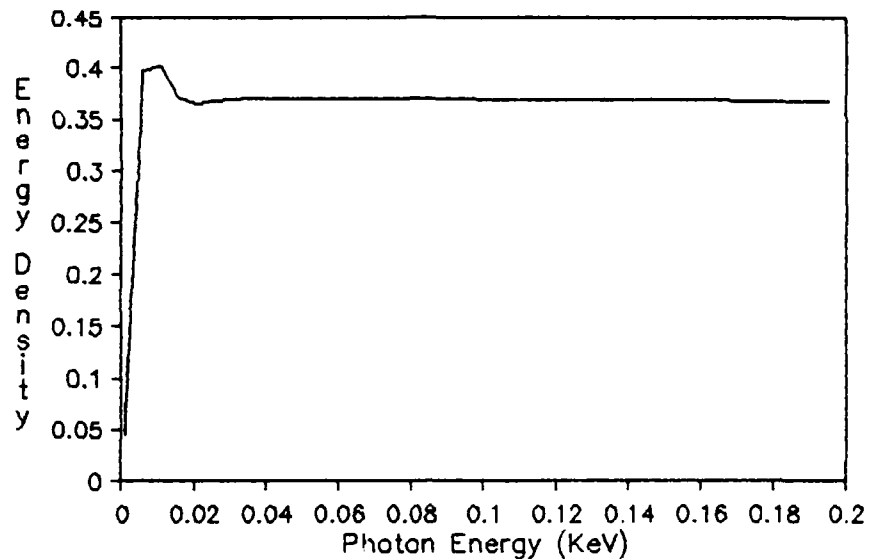


Fig. 4. Model 1 Time-Integrated Spectrum (Magnified View) Normalized to Unit Area; $\theta_1 = 1$ KeV

Actually, $E=0.001$ was the value for the lower integration limit in equation (28) for this example. The curve would in fact continue to approach zero at the left end as E approaches zero. The use of $E=\theta_1/1000$ instead of another value even closer to zero is justified because the approximately triangular-shaped area to the left of the curve from the ordinate value of 0.37 down to zero would be a negligible addition to the area under the curve ($1/2 \times 0.37 \times 0.01 = 0.00185$ or about 0.2% compared to 1). The small peak at the left end in Figure 4 is an artifact of the

calculation that becomes more narrow and displaced to the left as the temperature mesh, $\Delta\theta$, is made smaller, so in essence, it may be disregarded.

Spectra for initial temperatures of 0.02 and 10 KeV are shown, respectively, in Figures 5 and 6. Comparison of all three time-integrated spectra reveals, in general, that the spectrum shifts toward lower energies for lower initial temperatures and toward higher energies for higher initial temperatures, the same as for single-temperature Planckians. For instance, considering the areas under the curves, practically 100% of the total energy is carried away from the plasma by photons in the range 0 to 1 KeV when $\theta_i=0.02$ KeV, about 33% of the energy when $\theta_i=1$ KeV, and only 3% when $\theta_i=10$ KeV. Another feature of the time-integrated spectra similar to Planckian spectra is the fact that nearly all of the internal energy is radiated away by photons having energies less than $10\theta_i$ KeV.

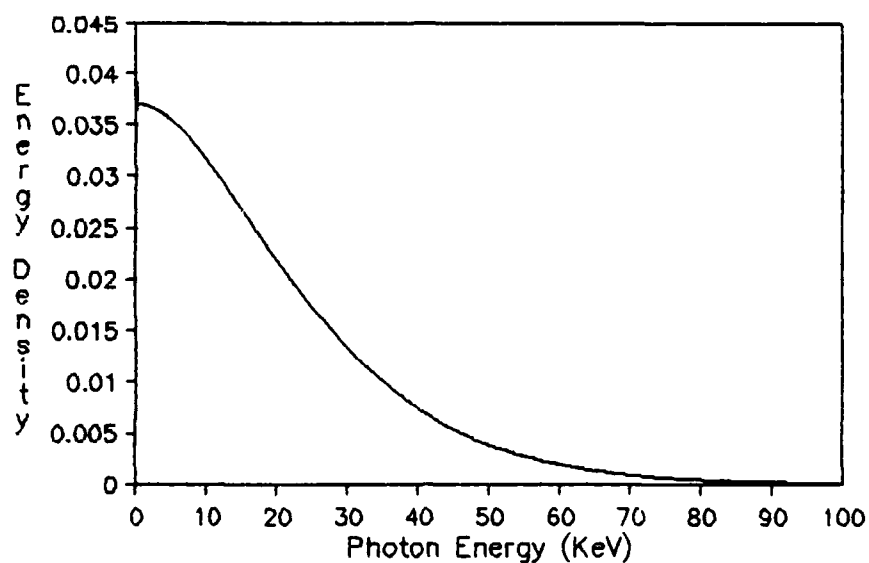


Fig. 5. Model 1 Time-Integrated Spectrum
Normalized to Unit Area; $\theta_1=10$ KeV

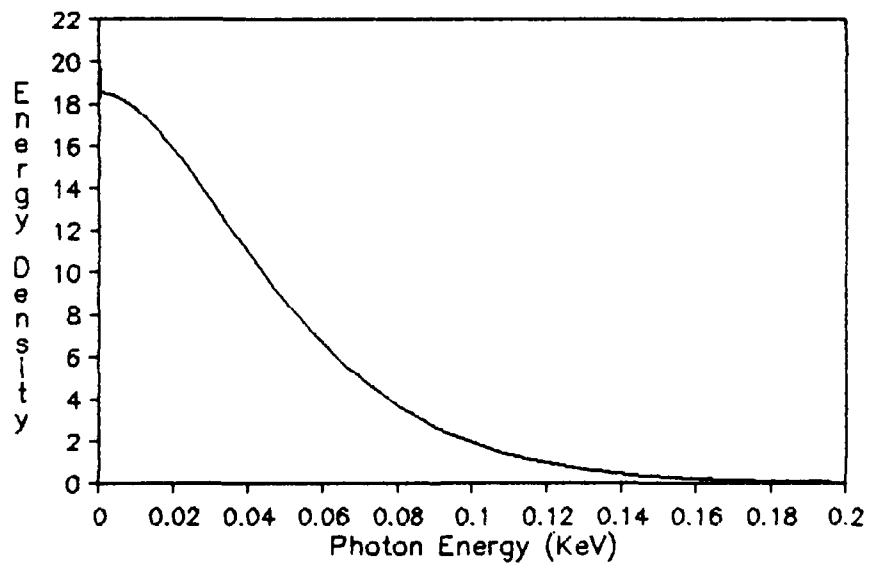


Fig. 6. Model 1 Time-Integrated Spectrum
Normalized to Unit Area; $\theta_1=0.02$ KeV

Significant differences between the two types of spectra
are the fraction of energy radiated at the lower end of the

spectrum and the most probable energy for photons. For any Planckian, approximately 1/30 of the total plasma energy is radiated at energies below its temperature, θ KeV, whereas for any Model 1 time-integrated spectrum, about ten times the Planckian fraction or one third of the total energy is radiated at energies below its initial temperature, θ , KeV. Over time, the most probable energy for photons of a constant temperature Planckian emitter is $E=2.82\theta$, corresponding to the energy location of the peak. For the cooling Planckian emitter, the most probable energy for photons shifts toward lower energies over time, the time-integrated spectrum showing it near $E=0$.

Summary

Model 1 represents an upper bounding case for energy density at the low end of the spectrum for the cooling Planckian emitter. With all of its energy in the form of material kinetic energy and the heat capacity remaining constant throughout the cooling process, there is an upper limit to the fraction of total energy radiated at the lower end of the spectrum. It turns out that density does not affect the normalized spectrum, as long as there exists some amount of material. If material energy constitutes a significant portion of the total energy of a cooling body, its most influential effect on the time-integrated spectrum would be seen at lower temperatures at the lower end of the spectrum.

In the next chapter we look at a model of the cooling plasma containing only radiation energy to observe its effects upon the fluence spectrum.

V. Model 2 - Radiative Cooling with Temperature Consistent,
Radiation Heat Capacity, but No Material Heat Capacity

We looked at the effect of including only material energy in the cooling emitter in the last chapter. Now we take a look at the effect of including only radiation energy.

Model 2 Description

The second model deals with the plasma cooling through the loss of radiation energy only. Either the material particles are at rest, with their kinetic energy being close to zero (but this would assume the body has already cooled to a temperature near 0 KeV), or else the material energy density is negligible compared to the radiation energy density at higher temperatures, which is more likely the case. At very high temperatures, well above the point where the atoms completely ionize, a drop in temperature to a point still above complete ionization would result in no change in heat capacity due solely to ionization. So this model seems appropriate at very high temperatures. Nevertheless, the model is extended to low temperatures to observe the cooling behavior there also, and binding energy is not taken into account.

Heat Capacity

The heat capacity in this approximation is dependent on temperature because of the high degree of dependence that $U_r(\theta)$ has on temperature. The form for radiation energy density is:

$$u_r(\theta) = U_r(\theta)/V = \alpha\theta^4 \quad (29)$$

where α is the radiation constant equal to $8.56E+28$ in units of $1/(\text{KeV-m})^3$ (3:22). The heat capacity is then:

$$C_v(\theta) = C(\theta)/V = du_r(\theta)/d\theta = 4\alpha\theta^3 \quad (30)$$

Replacing $C(\theta)$ in equation (23) with $C_v(\theta)$ and bringing the constant, 4α , outside the integral in the numerator and denominator of equation (24), it is seen that the constants cancel to give:

$$\hat{s}(E) \approx \frac{\int_{\theta_f}^{\theta_1} \rho(E;\theta)\theta^3 d\theta}{\int_{E_{\text{low}}}^{E_{\text{high}}} \int_{\theta_f}^{\theta_1} \rho(E;\theta)\theta^3 d\theta dE} \quad (31)$$

Note that $C_v(\theta)$ could just as well be θ^3 without loss of generality, which is the form of heat capacity used to calculate the fluence spectrum for Model 2.

Because the heat capacity has a θ^3 dependence, more energy is released from the plasma volume per degree drop in temperature at higher temperatures than at lower ones. Photons of higher energy should carry away more of the total energy than in the case of constant material heat capacity.

Correspondingly, the peak of the spectrum should, in general, shift toward higher energies, but the overall spectrum behavior must be determined from the heat capacity in conjunction with the function $\phi(E;\theta)$.

Time-Integrated Spectra

Predicting the shape of the spectrum can be done by examining the integrand in the numerator of equation (31) with $\phi(E;\theta)$ defined in equation (25):

$$\phi(E;\theta) \theta^3 = \frac{15}{\pi^4} \left[\frac{E^3}{\theta (e^{E/\theta} - 1)} \right] \quad (32)$$

In the limiting case at the low end of the spectrum, with $E=\theta$ and E approaching zero, the entire expression is constant except for a remaining E^2 term in the numerator. Therefore, as E^2 approaches zero, the integrand approaches zero. At the high end of the spectrum with $\theta < \theta_1 < \infty$, and E approaching infinity, the exponential in the denominator approaches infinity faster than the numerator; hence, the integrand again approaches zero. In between the two limits, a peak should occur at the same most probable energy as a Planckian with fixed temperature θ ($E=2.82\theta$), and the entire curve is scaled in height by the parameter θ^3 , as seen in the left hand side of equation (32).

Figure 7 shows the effect of adding several of the functions given by equation (32) for a few different temperatures. Curve d simulates approximately what the fluence spectrum might look like for a cooling body with a starting

temperature of 1 KeV. Notice that the peak has shifted to a higher energy as discussed above, but is left of the peak for a Planckian with temperature θ_1 . The second condition follows from the fact that as the body cools the energy distribution shifts to lower energies. Photons are most likely to have energies that are nearly equivalent to the body temperature.

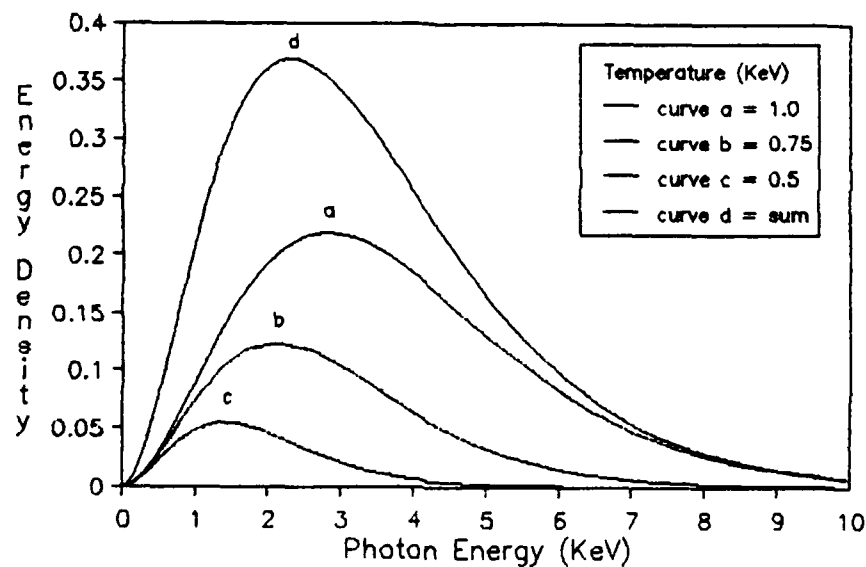


Fig. 7. Planckian Spectra a - c Normalized to Unit Area and Multiplied by θ^3

Furthermore, the second condition means there is an upper limit to the fraction of total energy that can be radiated at the high end of the spectrum. For example, a Planckian with temperature θ_1 KeV radiates a maximum of about 95.6% (or $29/30$) of the total energy at photon energies higher than θ_1 KeV. This upper limit should hold true for any time-integrated spectrum.

The time-integrated spectra for Model 2 are calculated from equation (31), again using the computer program in Appendix A with the subroutine for computing heat capacity changed to reflect $C_v(\theta)=\theta^3$. Figures 8 - 10 depict the calculated spectra with the same three initial temperatures used in Model 1. (Figure 10 also includes a comparison with Planckian spectra, which is discussed shortly.)

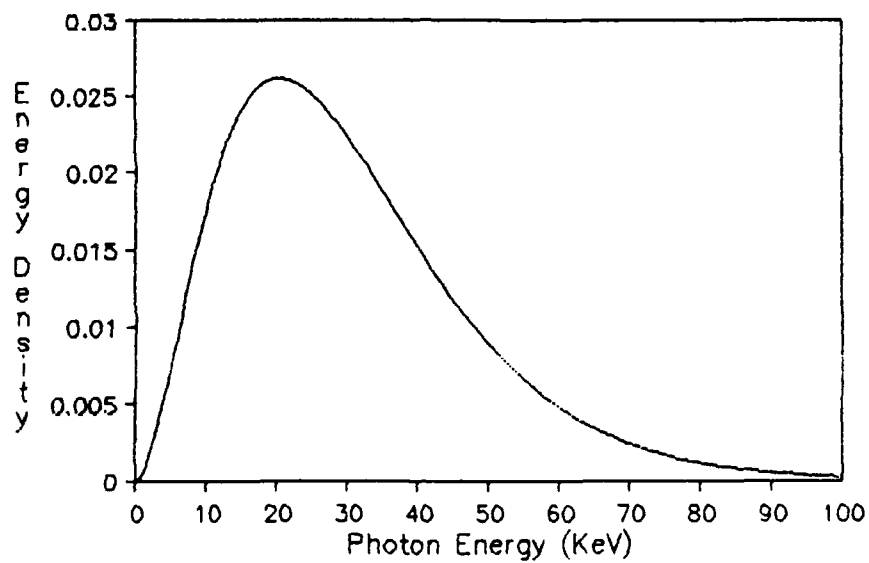


Fig. 8. Model 2 Time-Integrated Spectrum
Normalized to Unit Area; $\theta_i=10$ KeV

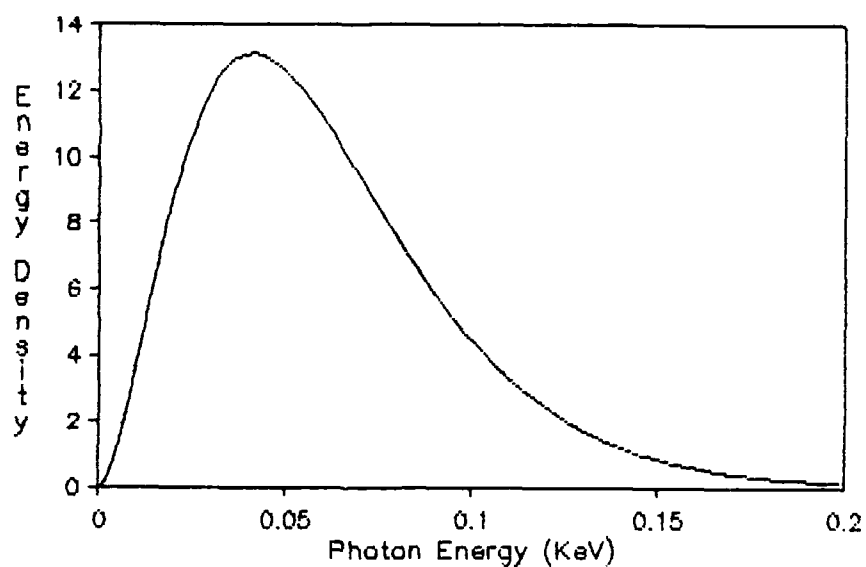


Fig. 9. Model 2 Time-Integrated Spectrum
Normalized to Unit Area; $\theta_1 = 0.02$ KeV

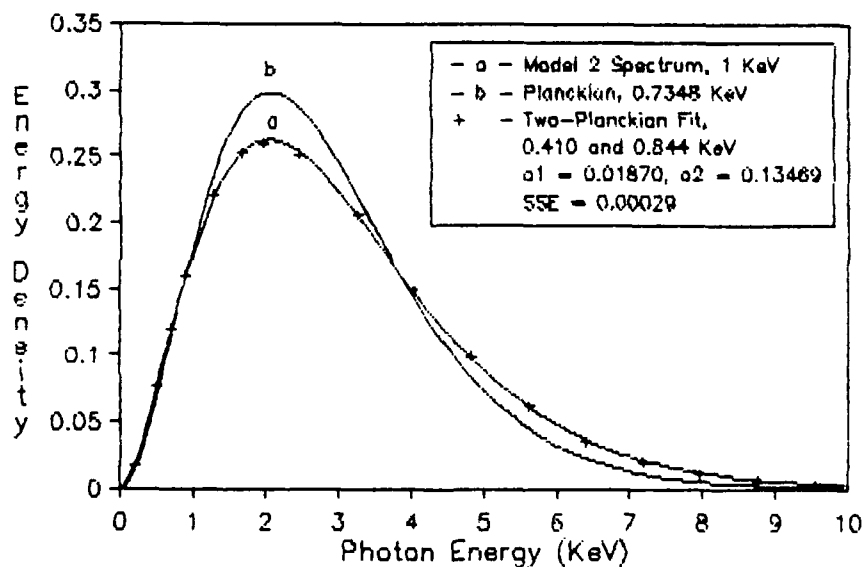


Fig. 10. Comparison of Time-Integrated Spectrum
 $\theta_1 = 1$ KeV with Plankian Spectra

All three time-integrated spectra have the same shape on a relative scale, but are located at different points if

placed on the same scale. The same trend occurs as in Figure 1 where the hotter spectra have more of their energy density at higher photon energies. Their peaks are smaller to accommodate the same area under the curves, and shifted to the right, to reflect the most probable energies being within a factor of three from the starting temperatures. Just the opposite is true of the colder spectra; the peaks grow taller and shift to the left for the same reasons.

Comparison with Planckian Spectra

Consider the time-integrated spectrum in Figure 10 with a starting temperature of 1 KeV. The shape of the spectrum is similar to a Planckian, but as anticipated, the peak is displaced to the left of that for a 1 KeV Planckian (the Planckian shown is one having $\theta = 0.7348$ KeV). The peak for the time-integrated spectrum is located at $E = 2.07\theta$, compared to $E = 2.82\theta$, for the corresponding Planckian peak, and the cooling body radiates about 92% of its total energy at energies above $E = \theta$, compared to 96% for the Planckian emitter always at a constant temperature.

Figure 10 shows the difference in shape between both types of spectra having both their peaks at the same energy, E . It can be seen that one Planckian roughly fits the time-integrated spectrum, whereas a combination of two Planckians with different temperatures practically matches

the spectrum. Appendix B contains a computer program to do the curve fitting using two Planckian basis functions. The equations for the fit are given by:

$$P_1(E) = E^3 / [\exp(E/\theta_1) - 1] \quad (33)$$

$$P_2(E) = E^3 / [\exp(E/\theta_2) - 1] \quad (34)$$

$$\S_{fit}(E) = \alpha_1 P_1(E) + \alpha_2 P_2(E) \quad (35)$$

The measure of the fit is given by the sum of the square of the errors:

$$SSE = \sum_E (\S(E) - \S_{fit}(E))^2 \quad (36)$$

where $\S(E)$ is the time-integrated spectrum value from equation (24), and $\S_{fit}(E)$ is the curve-fit value given by equation (35). From this result, the cooling body can be thought of as radiating at two temperatures, both below the initial temperature, instead of many temperatures over the course of time.

Summary

Model 2 represents an extreme bound in the opposite direction to Model 1. It shows there is an upper limit to the fraction of total energy that can be radiated at the high end of the spectrum. If the cooling body contains a significant portion of radiation energy, its effect would be seen at higher temperatures and energies than the case for constant material heat capacity, and in fact should be the dominant factor at the high temperatures and energies under

consideration, as will be seen in the next two chapters.

VI. Model 3 - Radiative Cooling with Constant, Material Heat Capacity and Temperature Consistent, Radiation Heat Capacity

This chapter combines the effects of both material and radiation energy in the cooling body. In the previous two models, temperature is the only parameter that influences the energy distribution, but now density becomes important, as we shall see.

Model 3 Description

The third model for the cooling body takes into account the loss of kinetic energy from the material particles and the loss of radiation energy or those photons that escape any further interaction within the plasma. This model could be valid at low temperatures and at very high temperatures, but excludes the range of intermediate temperatures where the ionization state of the atoms is changing with temperature. Binding energy is not included, but the intermediate range of temperatures is, so that, as before, cooling behavior can be observed here too. The densities considered may be somewhat high for plasmas in fusion experiments; however, they are chosen to illustrate noticeable effects for spectra with initial temperatures of 0.02 and 1 KeV.

Heat Capacity

Both the formula for material energy density from Model 1 and the formula for radiation energy density from Model 2 comprise the total internal energy density for Model 3:

$$u(\theta) = U(\theta)/V = u_m(\theta) + u_r(\theta) \quad (37)$$

$$= N_v(3/2)\theta + \alpha\theta^4 \quad (38)$$

Notice here why the effect due to material energy is dominant at low temperatures, and the effect due to radiation energy is dominant at high temperatures. Both N_v and α are about the same order of magnitude for nominal material densities, but θ^4 is much less than θ for $\theta \ll 1$ KeV, and it is much greater than θ for $\theta \gg 1$ KeV. The two terms are equal at approximately $\theta = 0.56$ KeV (6.5 million K) when $N_v = 1E+28$ atoms/m³.

The derivative of equation (38) with respect to temperature is the expression for heat capacity for Model 3:

$$C_v(\theta) = C(\theta)/V = du(\theta)/d\theta \quad (39)$$

$$= N_v(3/2) + 4\alpha\theta^3 \quad (40)$$

Time-Integrated Spectra

Substituting $C_v(\theta)$ for $C(\theta)$ in equation (24) results in the equation to compute the time-integrated spectrum for this model:

$$\mathfrak{A}(E) \approx \frac{\int_{\theta_f}^{\theta_i} \mathfrak{P}(E;\theta) C_v(\theta) d\theta}{\int_{E_{low}}^{E_{high}} \int_{\theta_f}^{\theta_i} \mathfrak{P}(E;\theta) C_v(\theta) d\theta dE} \quad (41)$$

All the spectra for Model 3 are calculated from equation (41) using the computer program in Appendix A, with the subroutine to compute heat capacity changed to reflect $C_v(\theta)$ in equation (40).

The predicted cooling behavior depends on the temperature. At high initial temperatures, most of the energy loss is due to the change in internal radiation energy. Therefore, the heat capacity has an almost pure θ^3 dependence like that of Model 2, so the spectrum should resemble a Model 2 spectrum with the same high initial temperature. The peak, however, should be displaced more to the left because as the plasma cools, more energy is lost from material than would be the case for radiation only. Such is the case for the 10 KeV spectrum of a plasma with density equal to $1E+27$ atoms/m³; however, the shift is too small to show any appreciable difference with the Model 2 spectrum in Figure 8. For low initial temperatures, most of the energy loss is due to the change in material energy. The heat capacity is nearly constant and becomes more so as the plasma cools. In this case, the spectrum should resemble a Model 1 spectrum having the same initial temperature, but with the peak shifted right because of the energy losses from internal radiation at temperatures closer to the initial temperature. The 0.02 KeV spectrum behaves thus, but again has a shift too small to show; it is almost identical to the spectrum in Figure 9 in Chapter V.

Cooling behavior from intermediate starting temperatures should show noticeable effects due to both material and radiation energy. The peak should fall between those of the pure material case and the pure radiation case for the same starting temperature. Figure 11 gives an example of this behavior, with the Model 3 spectrum calculated for a plasma density of $1E+29$ atoms/m³.

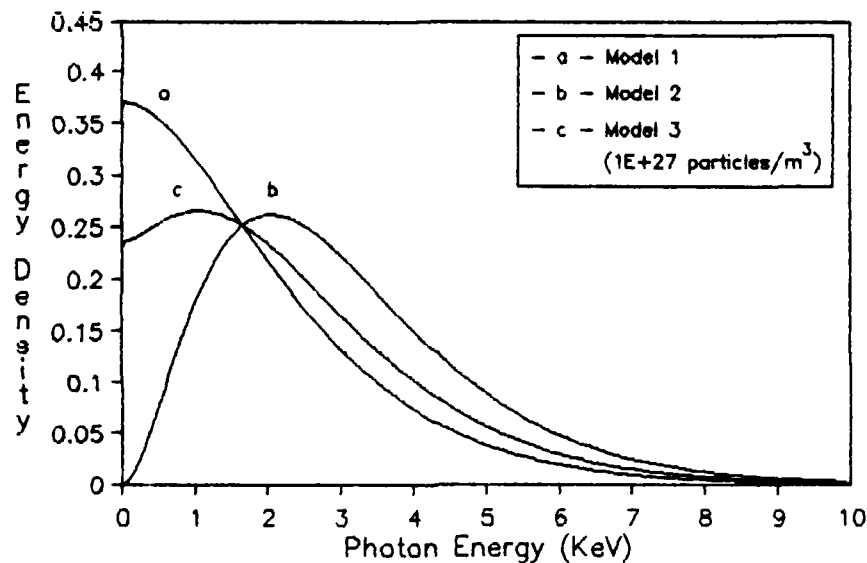


Fig. 11. Model 1, 2, and 3 Time-Integrated Spectra
Normalized to Unit Area; $\theta_i = 1$ KeV

Note that the left end of the Model 3 spectrum approaches a value greater than zero because of the material contribution to the loss of energy. This becomes more pronounced for colder θ_i , while for hotter θ_i the value approaches zero.

The predicted cooling behavior depends on density as well. Higher densities mean more material energy which forces the heat capacity to become more constant in nature

beginning at higher temperatures. The effect of increasing the density causes the lower end of the spectrum to approach its peak limiting value for pure material energy, as shown in Figure 12. A density of $1\text{E}+29$ (not shown) versus $1\text{E}+27$ atoms/ m^3 resulted in no noticeable change in the spectrum. See Figure 6 in Chapter IV for the limiting case.

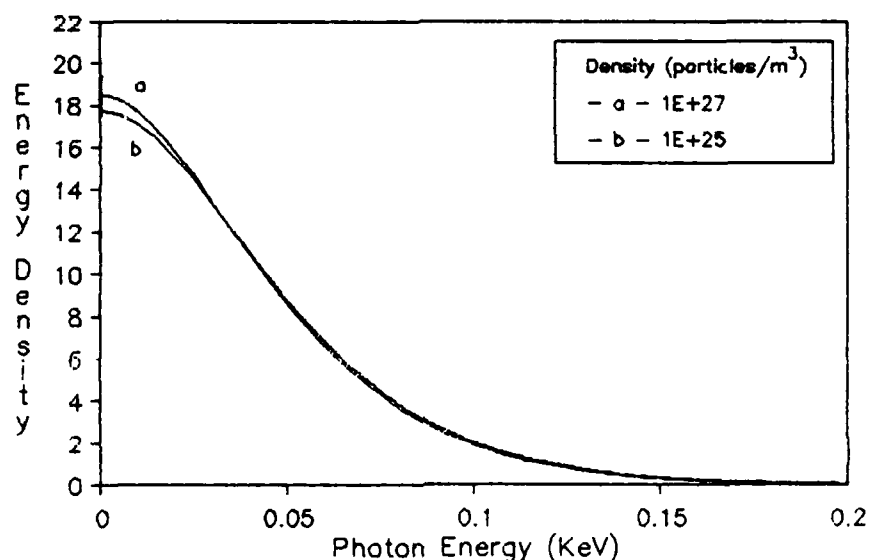


Fig. 12. Density Effect on Model 3 Time-Integrated Spectra Normalized to Unit Area;
 $\theta_i = 0.02$ KeV

Lower densities mean less material energy, and the nature of the heat capacity becomes more like the case for pure radiation. Figure 13 is a better example of what lowering the density does; the spectrum becomes more like the pure radiation case shown in Figure 11, or Figure 10 in Chapter V.

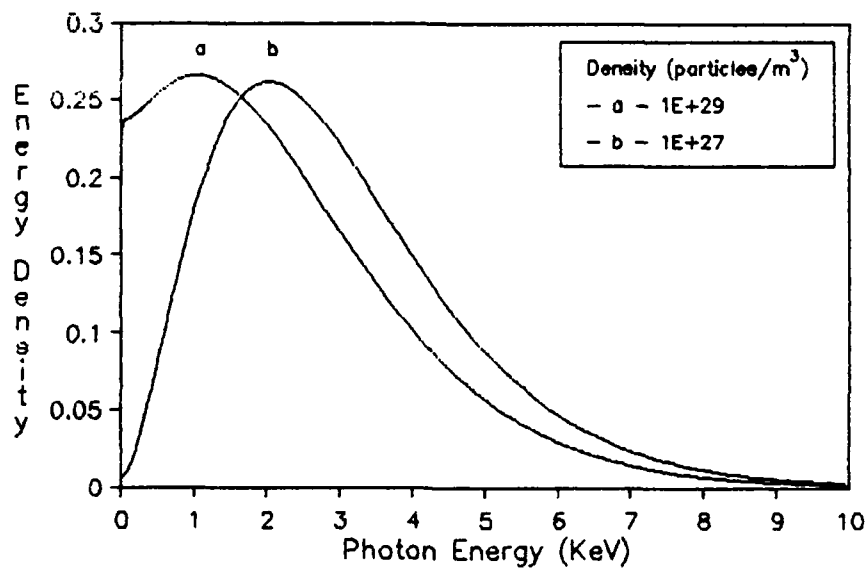


Fig. 13. Density Effect on Model 3 Time-Integrated Spectra Normalized to Unit Area;
 $\theta_i = 1$ KeV

Comparison with Planckian Spectra

Chapter V showed that two Planckian basis functions fit the fluence spectra of Model 2 much better than a single basis function. This is generally true for any spectrum having a shape closely resembling that for the pure radiation case. However, the curve-fit becomes worse for low temperature or high density Model 3 spectra as they become similar in shape to Model 1 spectra. Figures 14 and 15 support these conclusions for different densities.

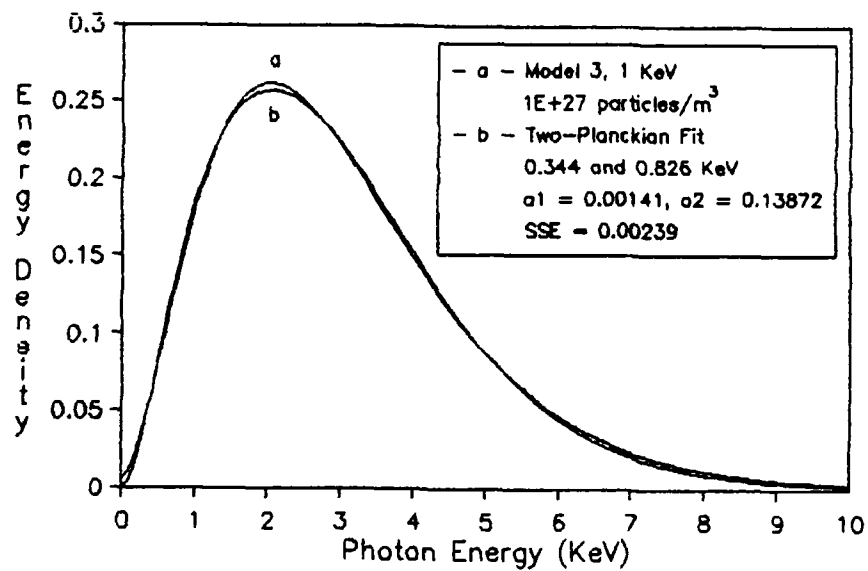


Fig. 14. Comparison of Two-Planckian Curve-Fit with Model 3 Spectrum; $N_v = 1E+27$ particles/m³

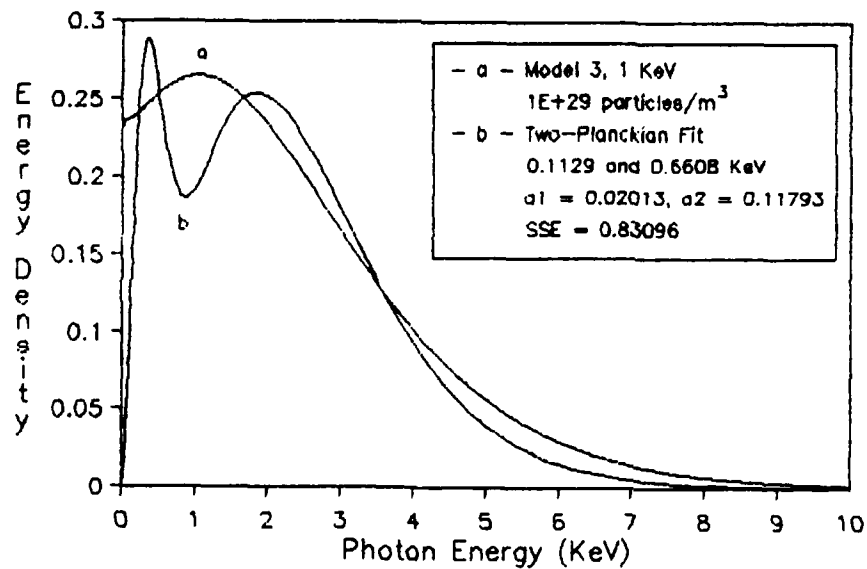


Fig. 15. Comparison of Two-Planckian Curve-Fit with Model 3 Spectrum; $N_v = 1E+29$ particles/m³

Summary

Model 3 represents a more realistic theory of cooling behavior between the extreme bounds of Model 1 and 2. The fluence spectrum generated by Model 3 combines effects of both material and radiation energy losses which place the most probable energy somewhere between the two extremes, depending on density and initial temperature of the plasma. In the case of high densities or low temperatures, Model 3 degenerates into the same behavior as Model 1; the heat capacity is nearly constant. At low densities or high temperatures, it becomes like Model 2; the heat capacity behaves as θ^3 . Although more realistic, this model is simplistic and incomplete without taking into account the release of energy as the ionization state falls for the ions in the cooling plasma. This aspect is covered in the next chapter.

VII. Model 4 - Radiative Cooling with Temperature Consistent Heat Capacity

Model 4 concentrates on how material composition affects the fluence spectrum of the cooling Planckian emitter. The form of material energy presented in Model 1 is changed to reflect the variable number of free electrons present in the plasma as the temperature falls and they bind to the ions. Binding energy is accounted for in yet another internal energy term to calculate the heat capacity. The results include variation in initial temperature and type of single element material, but the general effect due to variation in initial density is left to the previous chapter.

Model 4 Description

The fourth model describes the cooling plasma through the loss of three types of internal energy: material energy, radiation energy, and binding energy, all functions of temperature. As the temperature falls, free electrons in the plasma lose kinetic energy and are captured through electrostatic attraction by the ions, which eventually fill all electron shells to become neutral atoms. The shell structure is governed by:

$$n_{e,j} = 2j^2, \quad j=1,2,\dots \quad (42)$$

where $n_{e,j}$ is the total number of electrons allowed in principal quantum state j . Electrons are assumed to fill inner vacancies first and move progressively away from the nucleus

to fill outer vacancies last. When an electron is captured, it proceeds directly to the next unfilled vacancy, emitting a photon of energy equal to the absolute difference between the energy level of the vacancy just filled and the continuum. No allowance is made for intermediate excited states. The entire population of ions is considered to be at the same ionization state; however, fractional numbers of bound electrons are permitted to account for a distribution of ionization states encountered in real physical situations. This model applies primarily for all temperatures above the point where the material vaporizes. But as long as the initial temperature is hot enough to include some degree of ionization, then energy losses attributable to latent heats of vaporization and fusion are negligible compared to binding energy, and the model is valid at all temperatures. There is a restriction, however, on the upper limit for density, depending on type of material, because Model 4 uses a form of the Saha equation that assumes the free electrons are nondegenerate.

Binding Energy

Model 4 assumes the binding energy for outer electrons is less than that for inner electrons, which is consistent with the idea that inner electrons partially mask the attractive force of the nucleus. The energy level or ionization potential for each bound electron is determined from the following equation (3:170):

$$E_j = -I_H \left(\frac{Z_j^*}{j} \right)^2 + \frac{n_f e^2}{2R} \left(\frac{18}{5} - \frac{\overline{(r^2)}_j}{R^2} \right), \quad j=1,2,\dots \quad (43)$$

where I_H is the ionization potential for an electron in the ground state of a hydrogen atom; Z_j^* is the effective nuclear charge as seen by the electron in the j th energy state; n_f is the number of free electrons per atom; e is the electronic charge of an electron; R is the radius of the spherical region surrounding the ion which contains zero net charge, i.e., n_f free electrons; and $\overline{(r^2)}_j$ is the mean square radius of the electron orbit. The left hand term gives the energy levels for a hydrogen-like atom with atomic number Z_j^* , while the right hand term corrects for interactions between bound and free electrons, free electrons with the ion, and free electrons with free electrons, and adjusts the zero energy level so that all free electrons within the ion sphere maintain positive energy. (Bound electrons have negative energy). For convenience, equation (43) computes E_j in units of eV instead of Rydbergs if $I_H = 13.61$ eV and the right hand term is multiplied by $1/[4\pi\epsilon_0(1.602E-19 \text{ J/eV})]$, with ϵ_0 , the vacuum permittivity, in F/m and R in meters. The equation for effective nuclear charge is (3:168):

$$Z_j^* = Z - \sum_{k \neq j} n_k \sigma_{kj} - n_f \left(1 - \frac{1}{2j^2} \right) \sigma_{ff} \quad (44)$$

where Z is the element atomic number; n_k and n_f are the number of electrons in the corresponding shells screening

the nuclear charge from the electron in question; and σ_k , and σ_{ll} are Slater screening constants (3:169). To find the mean square radius (3:170):

$$\overline{(r^2)}_l = \frac{\alpha_0^2 j^4}{(Z_l^*)^2} \left(\frac{7}{4} + \frac{5}{4j^2} \right) \quad (45)$$

where α_0 is the first Bohr radius for the hydrogen atom in meters. Finally, the ion's sphere of influence has a radius given by the relationship (3:170):

$$\frac{4}{3}\pi R^3 = \frac{1}{N_v} \quad (46)$$

where N_v is the atomic number density.

From equation (43) and (46) it is seen that density is one factor that determines the binding energy, $-E_l$, required to remove the electron from the ion to become a free electron. A plot of binding energy, $-E_l$, versus density, N_v , in Figure 16 for the outer shell of electrons in carbon reveals that only densities less than $1\text{E}+28$ atoms/ m^3 satisfy the requirement that it takes more energy to remove the next electron than the previous one. Above this limit, the electron density is so high that the electrons become degenerate; that is, more than one electron occupies the same energy level. This upper density limit differs with atomic number Z , but for the four elements chosen, carbon, aluminum, copper, and plutonium, $N_v = 1\text{E}+27$ atoms/ m^3 is satisfactory for comparison of their spectra.

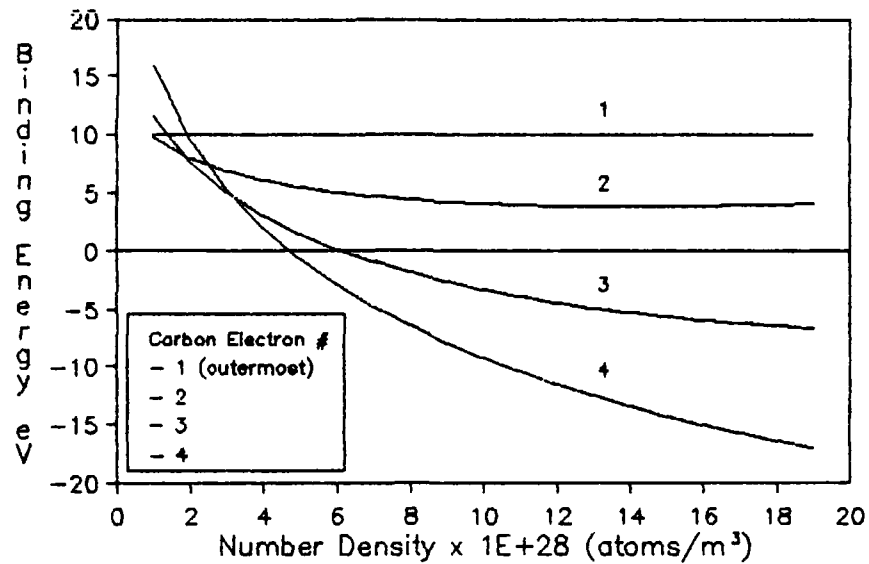


Fig. 16. Binding Energy versus Atomic Number Density for Carbon

The binding energy required to remove the outermost electron from an ion or neutral atom can be related to temperature by the following expression, taken from reference (4), which is derived from the Saha equation (3:164) for a plasma containing a single Z material:

$$e^{-E_j/\theta} = \left[\frac{2}{N_e} \left(\frac{2\pi m_e \theta}{h^2} \right)^{3/2} \right] / \left[\frac{2j^2}{n_j} - 1 \right], \quad j=1,2,\dots \quad (47)$$

$$N_e = n_r N_v \quad (48)$$

$$n_j = Z - n_r - \sum_j 2(j-1)^2 \quad (49)$$

where $m_e = 5.685E-15$ KeV-s²/m² is the mass of an electron; N_e is the electron density in 1/m³; $h = 4.136E-18$ KeV-s is Planck's constant; and E_j and θ are in KeV. If N_v and n_r are given, then E_j and θ can be calculated from equations (43) - (49). θ is the temperature that corresponds to n_r .

free electrons per atom. $-E_j$ is the energy needed to free the next electron to be added to the n_f free electrons. It is not included in the total binding energy required to remove n_f electrons, that is, the sum of the binding energies to remove each of the individual n_f electrons.

So at temperature θ , there are $N_v n_f$ free electrons per unit volume in the plasma, and the total binding energy is:

$$u_{be}(\theta) = U_{be}/V = -N_v \sum E_j(n_f(\theta)) \quad (50)$$

where the sum starts with 0 KeV for $n_f=0$ and adds the binding energy for each additional electron removed from the bound system. The function $n_f(\theta)$ is linearly interpolated from a table of values for n_f versus θ calculated from equations (43) - (49) for each element. A graph of n_f versus θ in Figure 17 for copper, that is typical of other elements, shows that equation (47) breaks down for transitions between electron shells when n_f approaches zero.

Because it is physically impossible to have more than one value of n_f electrons free from the atom at one temperature (which corresponds to one instant in time), the graph is smoothed as shown in Figure 18 by removing some of the points. In general, all elements have this "S"-shaped curve, and full ionization occurs at increasing temperatures for increasing Z .

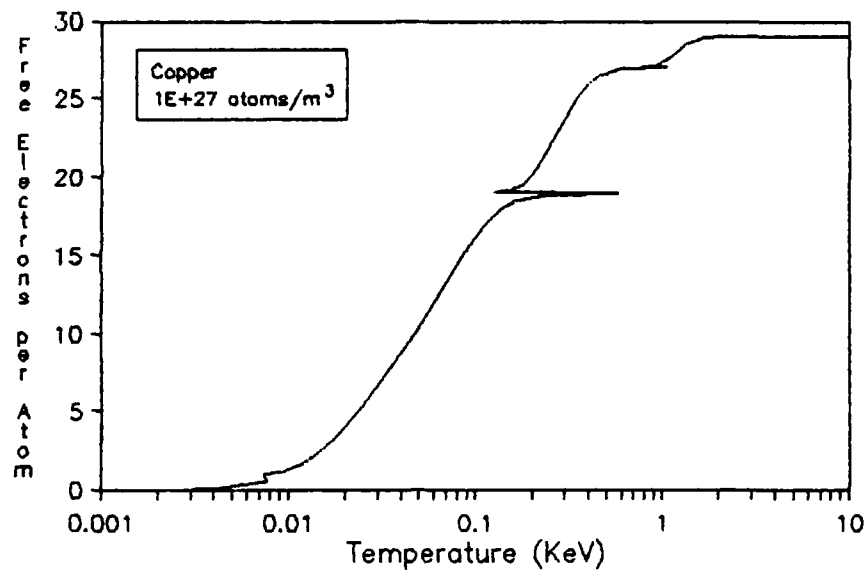


Fig. 17. Linear-Log Plot of Free Electrons per Atom versus Temperature for Copper

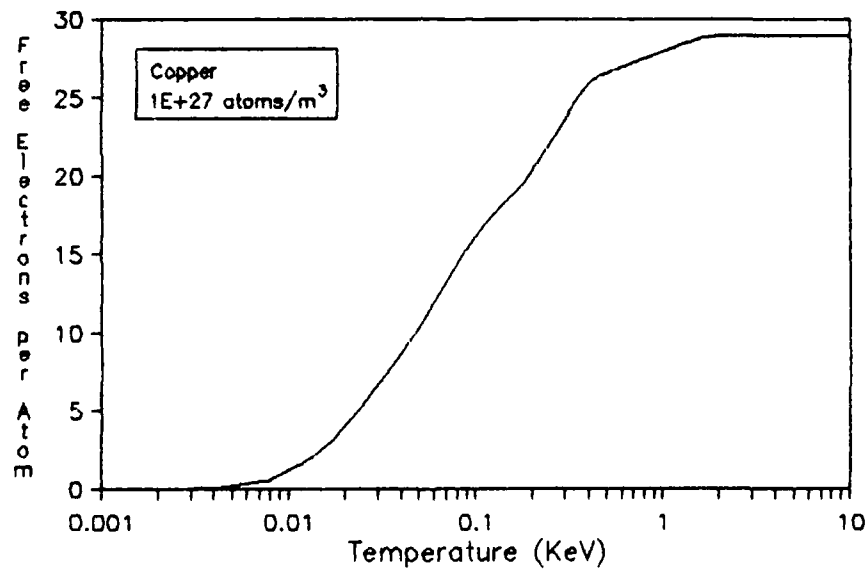


Fig. 18. Smoothed Linear-Log Plot of Free Electrons per Atom versus Temperature for Copper

The function of total binding energy versus number of free electrons per atom is linearly interpolated from a

table also. Examples of both tables are given in Appendix A for copper. A typical graph of total binding energy versus temperature is shown in Figure 19. All elements have this irregular, "S"-shaped curve, with the abrupt changes in slope caused by electron shell transitions and significant changes in slope from the corresponding free electron versus temperature curves. In general, total binding energy increases with temperature and increasing Z .

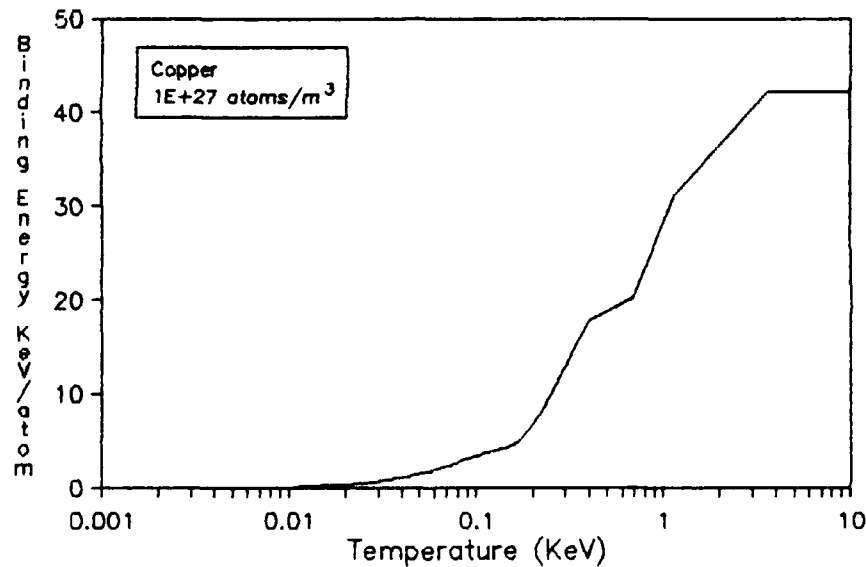


Fig. 19. Linear-Log Plot of Binding Energy per Atom versus Temperature for Copper

Appendix C has two computer programs to compute: 1) the binding energy for a particular electron, and 2) the corresponding temperature, from equations (43) - (49).

Material Energy

The material energy present in the plasma at any given time is dependent on the temperature and the number of free

particles which is decreasing because electrons bind to the ions as the temperature falls. Therefore, the material energy term is changed to reflect, in addition to the ions, the number of free electrons present as a function of temperature, with each particle having energy equal to $(3/2)\theta$:

$$u_m = N_v(1 + n_f(\theta))(3/2)\theta \quad (51)$$

Heat Capacity

The heat capacity is calculated from the expression for internal energy density which now has the form:

$$u(\theta) = N_v(1 + n_f(\theta))(3/2)\theta + a\theta^4 + N_v \sum [-E_i(n_f(\theta))] \quad (52)$$

Because $n_f(\theta)$ is different for every element and somewhat difficult to express as an analytical function, the derivative $du/d\theta$ is approximated by the change in internal energy over a small change in temperature $\Delta\theta$ as given by:

$$C_v = \frac{\Delta u}{\Delta \theta} = \left[u\left(\theta + \frac{1}{2}\Delta\theta\right) - u\left(\theta - \frac{1}{2}\Delta\theta\right) \right] / \Delta\theta \quad (53)$$

To get a feel for the magnitude of the change in binding energy compared to the change in material energy per temperature change of 1 KeV consider the graphs for copper again in Figures 18 and 19. In Figure 18, the number of free electrons at a temperature of 1 KeV is about 28, and at 0.03 KeV it is about 7. The change in material energy per KeV per atom, then, is:

$$\begin{aligned}\frac{\Delta u_m}{N_v \Delta \theta} &= \left[(1+28)\frac{3}{2}(1) - (1+7)\frac{3}{2}(0.03) \right] / (1-0.03) \\ &= 44 \text{ (KeV/KeV-atom)}\end{aligned}$$

In Figure 19, the binding energy at $\theta=1$ KeV is about 27 KeV, and at $\theta=0.03$ KeV it is 1 KeV. Hence, the change in binding energy per KeV per atom is:

$$\frac{\Delta u_{be}}{N_v \Delta \theta} = (27-1) / (1-0.03) = 27 \text{ (KeV/KeV-atom)}$$

The binding energy contributes approximately 60% as much change in energy to the heat capacity as does the material energy. For the other three elements, the ratio is approximately in the range of 30% - 110% . Thus, the change in binding energy is the same order of magnitude as the change in material energy.

Time-Integrated Spectra

The time-integrated spectra for Model 4 are calculated from equation (52) and (53) substituted into equation (41) from Chapter VI. Appendix A has the computer program to do this with the appropriate change to C_v in the subroutine to compute heat capacity.

The contribution to heat capacity from material energy in Model 4 is an order of magnitude or greater, depending on Z , than for Model 3, at temperatures above 0.1 KeV when the atomic number density N_v is the same. Add to this roughly the same contribution from binding energy, and the influence on the time-integrated spectrum due to the combined change

in material and binding energy is much greater than Model 3. The combined effect is most significant in the temperature range where most of the electron binding occurs, generally between 0.01 and 1 KeV for elements from carbon to plutonium. Spectra having initial temperatures of 1 KeV should show significant increases in energy density near the low end of the spectrum with a corresponding shift in the main peaks to the left, as compared to Model 3 spectra with the same density and temperature parameters. This also means the energy density should increase near the left end with increasing Z . Figure 20 portrays the results of four fluence spectra of differing material, with $\theta_i = 1$ KeV and the same atomic number density, $N_v = 1E+27$ atoms/m³.

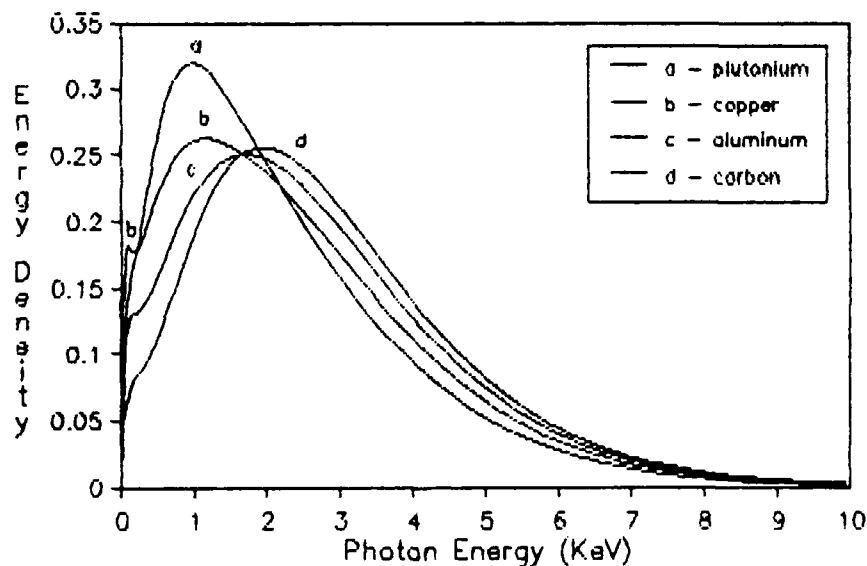


Fig. 20. Comparison of Model 4 Spectra
Normalized to Unit Area; $\theta_i = 1$ KeV,
 $N_v = 1E+27$ atoms/m³

One striking feature of these Model 4 spectra is evidence of a small peak or hump at low energies caused by the change in material and binding energy, but primarily binding energy. (This peak is not due to the same anomaly noted in Model 1 at the lower end of the spectrum because a smaller temperature mesh does not move the peak closer to $E=0$). The peak is more prominent for higher Z because more inner electrons bind per degree change in temperature, releasing more energy, than for lower Z . The exception in Figure 20 is plutonium, and the reason it has no prominent small peak is because the temperature does not start out hot enough to observe a rise in the change in binding energy to its greatest value between $\theta=1$ and 2 KeV as shown in Figure 21, although it does rise to its greatest change in the number of binding electrons between $\theta=0.02$ and 0.05 KeV, as shown in Figure 22.

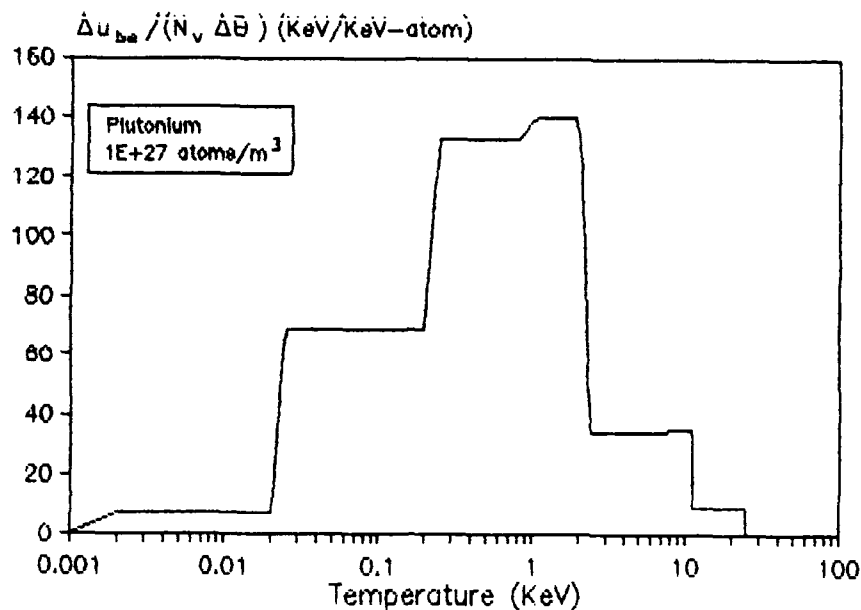


Fig. 21. Linear-Log Plot of Change in Binding Energy per Atom with Respect to Temperature versus Temperature for Plutonium

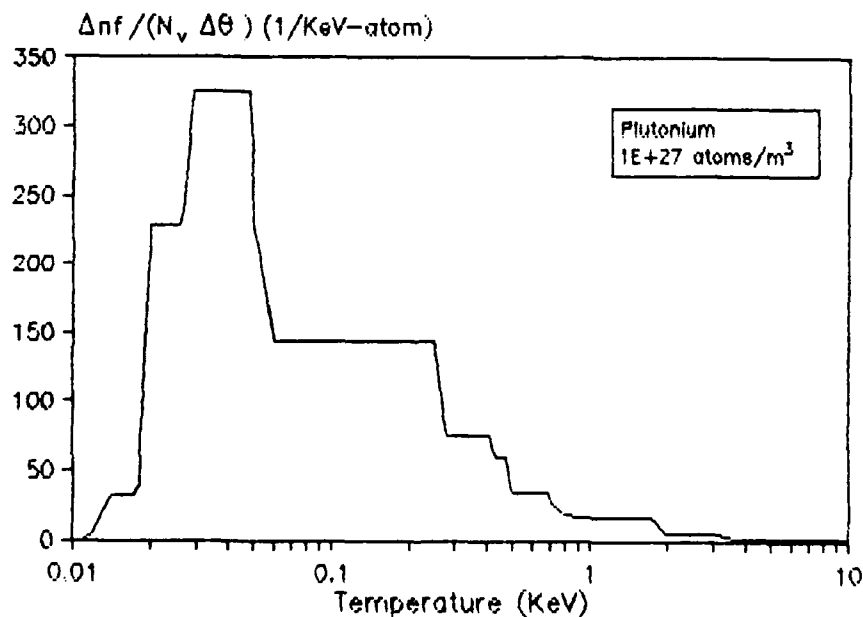


Fig. 22. Linear-Log Plot of Change in Free Electrons per Atom with Respect to Temperature versus Temperature for Plutonium

Spectra having initial temperatures much higher than 1 KeV show increasing tendency to become like Model 2 spectra because of the dominant effect of radiation energy at high temperatures where most of the energy is radiated. Spectra having initial temperatures below about 0.01 KeV become more like Model 1 spectra with constant material energy because all of the electrons are bound, eliminating any change in binding energy, and the change in radiation energy is too small compared to the change in material energy.

Comparison with Planckian Spectra

The result of a two-Planckian curve-fit for the Model 4 copper spectrum with starting temperature equal to 1 KeV and atomic number density equal to $1\text{E}+27$ atoms/ m^3 is displayed in Figure 23.

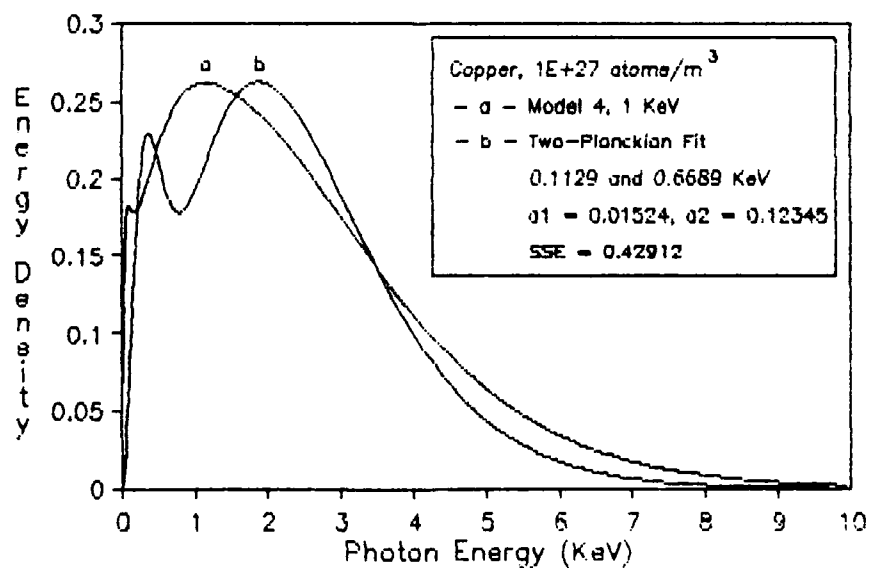


Fig. 23. Comparison of Two-Planckian Curve-Fit with Model 4 Spectrum

Again, the fit is not as good as higher temperature or lower Z spectra that look more like Model 2 spectra having only internal radiation energy. The fit is better for a particular Z material when its spectrum resembles the plutonium spectrum in Figure 20; that is, the initial temperature is equal to or lower than that at which the greatest change in binding energy occurs, with the density being sufficiently low, so that the lower end of the spectrum has no prominent small peak and approaches an energy density value close to zero.

A much better curve-fit is obtained by combining three Planckians and a Model 1 spectrum. Two Planckians are used to match the curve from the top of the main peak to the upper end of the spectrum, while a scaled Model 1 spectrum is used to match the majority of the curve from the lower end of the spectrum to the top of the main peak. The third Planckian is scaled to match the small peak. The result is shown in Figure 24 and compared to the Model 4 copper spectrum in Figure 25.

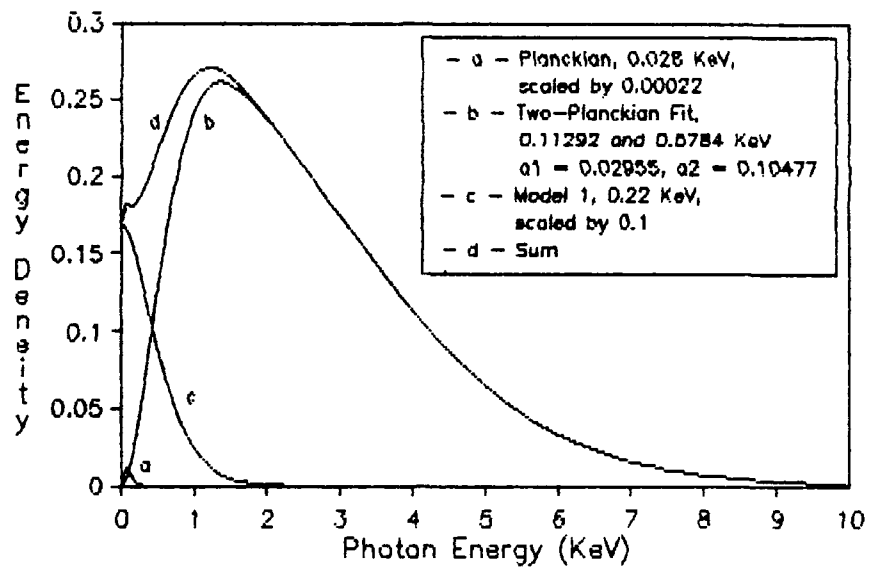


Fig. 24. Combination Curve-Fit for Model 4 Copper Spectrum

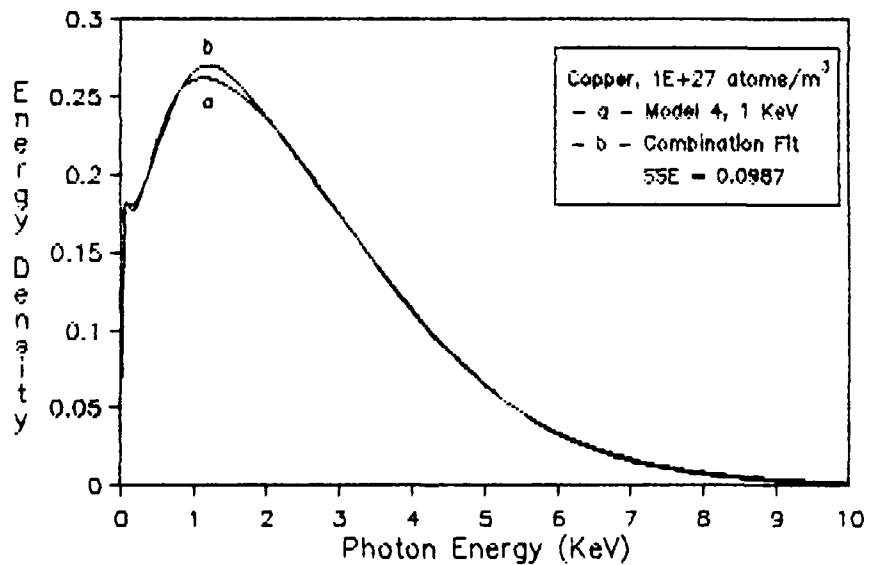


Fig. 25. Comparison of Combination Curve-Fit with Model 4 Copper Spectrum

Summary

Model 4 presents the most realistic case for the cooling Planckian emitter of the four models examined. It accounts for losses in material energy, radiation energy, and binding energy, the major contributors to internal energy, as the temperature falls. The cooling behavior of Model 4 may not be truly accurate because of the somewhat arbitrary smoothing of the free electron curves; however, it gives general trends in the spectra for changes in temperature, density, and material composition parameters. As the ionization state falls within the cooling plasma, the change in material and binding energy may produce a smaller peak in energy density at lower photon energies than the main peak caused primarily by the change in internal radiation energy, depending on initial temperature and density. If the initial temperature and density can be deduced and are in an appropriate range, the material composition might be recognized from its signature on the fluence spectrum, provided a detector has the resolution to differentiate the peaks.

VIII. Conclusions and Recommendations

The objective of investigating the nature of the time-integrated spectrum for a cooling Planckian emitter was approached by considering four models that dealt with the composition and change in internal energy radiated out through the surface of the emitter. The change in material, radiation, and binding energy taken separately or in combination, give insight to how these quantities determine the heat capacity, which in turn determines how much energy is released as the temperature drops. Three parameters were varied, temperature, density, and material composition, each of which changed the internal energy for some or all of the models. Also, a few selected spectra were compared with Planckian spectra to see if they could be fit with one or two Planckian basis functions.

Conclusions

This study of time-integrated spectra revealed the following conclusions:

- The most significant effect of material and binding energy is seen at lower photon energies of about 1 KeV or less, depending on initial temperature and density, and may produce a small peak or hump in the spectrum separate from the main peak. The material composition could be determined from this signature if the initial temperature and density are known.

- The fluence spectrum of a cooling Planckian emitter has a non-Planckian distribution of energy.
- Two Planckian basis functions fit fluence spectra from high initial temperature emitters best, or those that resemble Model 2 spectra, whereas the fit becomes poor for fluence spectra from high density emitters, or those that resemble Model 1 Spectra. In such case, the fit becomes better if more Planckian basis functions are used.

Recommendations

Further improvements to Model 4 can be made by including the effect of expanding volume on temperature and density, and also accounting for diffusion of energy from a hotter interior to a colder surface to approximate the true temperature at which radiation is emitted.

Appendix A: Computer Program to Calculate the Time-Integrated Spectrum

The following program calculates the time-integrated spectrum using the academic version of TK Solver Plus (5). The heat capacity is changed in the subroutine labeled RULE FUNCTION: C for the different models. A "C" at the far left edge indicates the equation is cancelled and is not used in computations, similar in effect to a comment line denoted with " .

===== VARIABLE SHEET ===== For Academic Use Only

St	Input	Name	Output	Unit	Comment
94		Z			Atomic number.
.02		0i		KeV	Initial temperature.
.00001		lowE		KeV	Lowest photon energy.
.01		highE		KeV	Highest photon energy.
500		0steps			Number of temperature steps (mesh).
100		Esteps			Number of energy steps (mesh).
					(Each mesh must be an even number for Simpson's rule of integration).
'Planck		func			Planck function on Function Sheet.
'Ionize		func2			Ionize function on Function Sheet.
50		ratio			E/0.
1E27		Nv		1/m^3	Number density.
		area	3.941E-8	KeV/m^3	Area under non-normalized spectrum.
					3.941044336095132E-8
5.896E-10		areal		KeV/m^3	Area 1 under non-normalized spectrum

for split energy mesh.

5.895735721927842E-10

1 mult Density multiplier.

===== RULE SHEET ===== For Academic Use Only

S Rule-----

Call blank('f) "blank erases array values.

Call blank('E)

Call blank('s)

Call Cool(func;area)

===== PROCEDURE FUNCTION: Cool ===== For Academic Use Only

Comment: Calculates spectrum.

Parameter Variables: lowE,highE,Esteps,θi,θsteps

Input Variables: func

Output Variables: F

S Statement-----

* Additional notation not included in VARIABLE SHEET:

* deltaE Energy interval.

* E Photon energy value.

* 'f[i] (An array). Value of the normalized Planck function
times heat capacity integrated over the appropriate temperature limits, with the ith E as an energy parameter.

* F Sum of all 'f[i] integrated over the appropriate energy
limits. (Area under non-normalized spectrum).

* k Multiplication factor = 1 or 2.

* 's[i] (An array). Normalized spectrum value = 'f[i] / F.

* value Intermediate function value.

° =====

° Check to see that energy mesh has even number of intervals.

° =====

IF MOD(Esteps,2)<>0 THEN error:= odd_number_of_intervals

° =====

° Integration over energy using Simpson's rule. Basic procedure is borrowed

° and modified from reference (5).

° =====

deltaE := (highE - lowE) / Esteps

E := lowE

k := 1

value := 0

FOR i := 2 TO Esteps

 E := E + deltaE

 k := 3 - k

 'f[i] := Simpson(func, 0i, 0steps, E)

 value := value + k * 'f[i]

NEXT i

'f[1] := Simpson(func, 0i, 0steps, lowE)

'f[Esteps + 1] := Simpson(func, 0i, 0steps, highE)

F := (2 * value + 'f[1] + 'f[Esteps + 1]) * deltaE / 3

° =====

" Calculate normalized spectrum and fill lists (arrays) for plotting.

" =====

E := lowE

FOR i := 2 TO Esteps + 1

 E := E + deltaE

 'E[i] := E

 's[i] := 'f[i] / F

NEXT i

'E[1] := lowE

's[1] := 'f[1] / F

===== PROCEDURE FUNCTION: Simpson ===== For Academic Use Only

Comment: Integration over temperature using Simpson's rule.

Parameter Variables: ratio, θ_i

Input Variables: func, high θ , θ steps, E

Output Variables: value

S Statement: _____

" Description: Standard method of numerical integration using second-degree

" polynomial approximation of integrand.

" Additional notation not included in VARIABLE SHEET.

" apply(func, a, b) Calls a named function (func) defining the

" integrand and supplies the appropriate arguments

" (a, b).

" delta θ Temperature interval.

" high θ Upper temperature integration limit.

- low0 Lower temperature integration limit.
- temp Temperature.
- value Intermediate function value and final value for inte-
- gration over temperature.

▪ =====

▪ Check to see that temperature mesh has even number of intervals.

▪ =====

IF MOD(0steps,2)<>0 THEN error:= odd_number_of_intervals

▪ =====

▪ Change lower temperature integration limit based on energy E and ratio of

▪ E/0. E/ratio must be lower than 0i.

▪ =====

low0 := E / ratio

IF low0 >= 0i THEN error := ratio_is_too_small

▪ =====

▪ Integration over temperature using Simpson's rule. Basic procedure is bor-

▪ rowed and modified from reference (5).

▪ =====

delta0 := (high0 - low0) / 0steps

temp := low0

```

k := 1
value := 0
FOR i := 2 TO 0steps
    temp := temp + delta0
    k := 3 - k
    value := value + k * apply(func, E, temp, delta0, low0, high0)
NEXT i
value := (2 * value + apply(func, E, low0, delta0, low0, high0) + apply(func,
    * E, high0, delta0, low0, high0)) * delta0 / 3

```

===== RULE FUNCTION: Planck ===== For Academic Use Only

Comment: Normalized Planck function.

Parameter Variables:

Argument Variables: E,0,delta0,low0,high0

Result Variables: p

S Rule_____

- * Additional notation not included in VARIABLE SHEET:
- * p Normalized Planckian times heat capacity.
- * planck Normalized Planckian value.

planck = 15 / (pi())^4 * E^3 / (0^4 * (EXP(E/0) - 1))

p = planck * C(0, delta0, low0, high0)

===== RULE FUNCTION: C ===== For Academic Use Only

Comment: Heat capacity.

Parameter Variables: Nv,0i,Z

Argument Variables: 0,delta0,low0,high0

Result Variables: heatcap

S Rule

* Additional notation not included in VARIABLE SHEET and previous functions.

*	a2	Radiation constant.
*	heatcap	Heat capacity.
*	ion1	Binding energy at temp1.
*	ion2	Binding energy at temp2.
*	ionize	Function that computes binding energy per atom.
*	material1	Material energy density at temp1.
*	material2	Material energy density at temp2.
*	rad1	Radiation energy density at temp1.
*	rad2	Radiation energy density at temp2.
*	starA	Intermediate Zstar function value.
*	starB	Intermediate Zstar function value.
*	star1	Zstar function value for temp1.
*	star2	Zstar function value for temp2.
*	temp	Intermediate temperature value.
*	temp1	Lower temperature of temperature interval.
*	temp2	Upper temperature of temperature interval.
*	temp3	Intermediate temperature value.
*	theta	Temperature value.
*	Zstar	Function that computes the number of free electrons per atom at a given temperature.

* =====

* For Model 1.

* =====

C heatcap = 1

▪ =====

▪ For Model 2.

▪ =====

heatcap = θ^3

▪ =====

▪ For Model 3.

▪ =====

C a2 = 8.5634E+28 *Radiation constant expressed in $1 \backslash (\text{KeV-m})^3$.

C heatcap = $N_v * (3 / 2) + 4 * a2 * \theta^3$

▪ =====

▪ For Model 4.

▪ =====

C a2 = 8.5634E+28 *Radiation constant expressed in $1 \backslash (\text{KeV-m})^3$.

▪ =====

▪ Determine lower and upper temperatures of interval.

▪ =====

C temp = $\theta - \text{delta}\theta / 2$

```

C IF  $\theta$  = low $\theta$  THEN temp1 = low $\theta$  ELSE temp1 = temp
C temp3 =  $\theta$  + delta $\theta$  / 2
C IF  $\theta$  = high $\theta$  THEN temp2 = high $\theta$  ELSE temp2 = temp3

```

```

* =====
* Determine number of free electrons per atom at both temperatures.
* =====

```

```

C starA = ABS(Zstar(temp1))
C IF starA > Z THEN star1 = Z ELSE star1 = starA
C starB = ABS(Zstar(temp2))
C IF starB > Z THEN star2 = Z ELSE star2 = starB

```

```

* =====
* Compute material energy density at both temperatures.
* =====

```

```

C matter1 =  $N_v * (1 + star1) * 3 / 2 * temp1$ 
C matter2 =  $N_v * (1 + star2) * 3 / 2 * temp2$ 

```

```

* =====
* Compute radiation energy density at both temperatures.
* =====

```

```

C rad1 =  $a_2 * temp1^4$ 
C rad2 =  $a_2 * temp2^4$ 

```

```

      * =====
      * Compute binding energy per atom at both temperatures.
      * =====

```

C ion1 = Nv * ABS(Ionize(star1))

C ion2 = Nv * ABS(Ionize(star2))

```

      * =====
      * Compute heat capacity for temperature interval.
      * =====

```

C heatcap = (matter2 + rad2 + ion2 - (matter1 + rad1 + ion1)) / delta0

===== LIST FUNCTION: Zstar ===== For Academic Use Only

Comment: Interpolation function for free electrons vs temperature.

Domain List: kT7a

Mapping: Linear

Range List: nf7a

Element— Domain— Range—

1	0	0
2	.00245345426244727	.01
3	.0040090803003785	.1
4	.00766489707885056	.5
5	.0113754622168454	1.5
6	.0133180652203634	2
7	.0168206934563477	3
8	.0240665353092386	5

9	.0475779982016186	10
10	.0857295777914731	15
11	.113199665581666	17
12	.177949883904736	19.5
13	.278790992266599	23
14	.348411231622957	25
15	.407371098297251	26
16	.465070257418233	26.5
17	1.36937648331806	28.5
18	1.70020947649073	28.9
19	2.12480361177458	28.98
20	2.36418313794776	28.99
21	3.62590540771914	29
22	10	29

===== LIST FUNCTION: Ionize ===== For Academic Use Only

Comment: Interpolation function for binding energy vs nf.

Domain List: nfCu

Mapping: Linear

Range List: bindCu

Element— Domain— Range—

1	0	0
2	1	.01055774
3	2	.10225568
4	3	.20641458
5	4	.32435908
6	5	.45741488

7	6	.60690848
8	7	.77416718
9	8	.96051848
10	9	1.16729018
11	10	1.39581038
12	11	1.64740738
13	12	1.92340938
14	13	2.22514478
15	14	2.55394218
16	15	2.91112998
17	16	3.29803688
18	17	3.71599148
19	18	4.16632238
20	19	4.65035818
21	20	6.26254918
22	21	7.96334218
23	22	9.75521318
24	23	11.64063918
25	24	13.62209718
26	25	15.70206518
27	26	17.88301918
28	27	20.16743618
29	28	31.01259618
30	29	42.09627618

Appendix B: Computer Program to Fit Time-Integrated Spectra
with Two Planckian Basis Functions

This program computes the best least squares approximation for a spectrum from a given range of temperatures and two Planckian basis functions. Its output gives the two Planckian temperatures and the coefficients necessary to calculate the curve, plus a measure of how good the fit is using the sum of the square of the errors or difference between original and calculated Y-axis values. The program is written in FORTRAN 77 language and calls a mathematical library routine DFNLSQ written by IMSL (6). Typical output follows the program.

* Maj Drew Fisher

* 14 Oct 89

PROGRAM PLANCK

* =====

* This program computes a least squares approximation with user-
* supplied basis functions. The approximation takes the form

*

* $Y = \text{COEFF}(1) + \text{COEFF}(2)*F(1,X) + \text{COEFF}(3)*F(2,X)$

* Definitions:

* COEFF - Coefficient array.

* COEFF2 - Storage array for coefficients.

* DELTAT - Temperature increment.

*	DFNLSQ	- Library routine that computes least
*		squares approximation with user-supplied
*		basis functions.
*	ENERGY	- Array of X-axis values.
*	F	- Subroutine for computing values from
*		basis functions.
*	FRACT	- Array of original Y-axis values.
*	INDEX1	- Stores index counter I.
*	INDEX2	- Stores index counter J.
*	INTCEP	- Intercept.
*	IWT	- Weight option (not used).
*	JJ	- A counter.
*	N	- Counter used for number of data points.
*	NBASIS	- Number of basis functions.
*	NFLIP	- Flip flop counter.
*	NSIZE1	- Array size.
*	NSIZE2	- Array size.
*	NUM1	- Loop index.
*	NUM2	- Loop index.
*	RESET	- Original TEMP1.
*	SSE	- Sum of squares of the errors - an indicator
*		of fit.
*	STORE	- Storage array for SSE.
*	TEMP1	- Stores temperature for first basis function.
*	TEMP2	- Stores temperature for second basis function.
*	THETA1	- Temperature for first basis function.

```

*          THETA2      - Temperature for second basis function.
*          WEIGHT      - Weights given to basis functions (an array of
*                        higher dimension if weights other than 1 are
*                        assigned).
*
*=====
INTEGER I, INDEX1, INDEX2, INTCEP, IWT, J, JJ, M, N, NBASIS
INTEGER NFLIP, NSIZE1, NSIZE2, NUM1, NUM2

  PARAMETER (IWT = 0, NBASIS = 2, NSIZE1 = 10, NSIZE2 = 200)
DOUBLE PRECISION COEFF(NSIZE1), COEFF2(NSIZE1), DELTAT
DOUBLE PRECISION ENERGY(NSIZE2), FRACT(NSIZE2), RESET, SSE
DOUBLE PRECISION STORE(2), TEMP1, TEMP2, THETA1, THETA2, WEIGHT

  PARAMETER (WEIGHT = 1)

COMMON THETA1, THETA2

EXTERNAL DFNLSQ, F
*
*=====
* Open file containing X-axis and Y-axis spectrum values.
*
*=====

OPEN (UNIT = 20, FILE = 'cufit', STATUS = 'OLD')

N = 1

10 READ (UNIT = 20, *, END = 20) ENERGY(N), FRACT(N)

  PRINT*, N, ENERGY(N), FRACT(N)

  N = N + 1

  GOTO 10

20 CONTINUE

```

```

N = N - 1

PRINT*

PRINT*, 'Number of points =', N

CLOSE (UNIT = 20)

*  =====
*  User input.
*  =====

PRINT*, 'Include intercept? (1 = Yes, 0 = No)'

PRINT*

READ*, INTCEP

PRINT*

PRINT*, 'For investigation, start THETA1 and THETA2 at'

PRINT*, 'what temperatures (KeV)? (THETA1, THETA2)'

PRINT*

READ*, THETA1, THETA2

PRINT*

PRINT*, 'Increment temperatures by what DELTAT?'

PRINT*

READ*, DELTAT

PRINT*

PRINT*, 'Loop information. How many iterations for each'

PRINT*, 'loop? (inside [THETA1], outside [THETA2])'

PRINT*

READ*, NUM2, NUM1

PRINT*

```

```

*      =====
*      Initialize values.
*      =====

NFLIP = 1

RESET = THETA1

STORE(1) = 1.0D+00

STORE(2) = STORE(1)

TEMP1 = THETA1

TEMP2 = THETA2

INDEX1 = 1

INDEX2 = 1

JJ = 0

*      =====
*      Start search for temperatures that give lowest SSE.
*      =====

DO 80 I = 1, NUM1

    PRINT*, 'I =', I

    THETA1 = RESET

    DO 70 J = 1, NUM2

        IF (THETA1 .NE. THETA2) THEN

            JJ = JJ + 1

            CALL DFNLISQ (F, INTCEP, NBASIS, N, ENERGY, FRACT, IWT,
$                               WEIGHT, COEFF, SSE)

```

```

*      =====
*      Store coefficients from first loop pass in
*      temporary storage.
*      =====

      IF (JJ .EQ. 1) THEN
        DO 40 M = 1, NBASIS + 1
          COEFF2(M) = COEFF(M)
40      CONTINUE
      ENDIF

      NFLIP = 3 - NFLIP
      STORE(NFLIP) = SSE

*      =====
*      Compare SSE with the old value of SSE and overwrite
*      temporary storage locations with the smallest value
*      and its associated values. Three cases are checked
*      and a fourth one implies no change.
*      =====

      IF (NFLIP .EQ. 2 .AND. STORE(2) .LT. STORE(1)) THEN
        STORE(1) = STORE(2)
        TEMP1 = THETA1
        TEMP2 = THETA2
        INDEX1 = I
        INDEX2 = J
        DO 50 M = 1, NBASIS + 1

```



```

                                COEFF2(M) = COEFF(M)
50      CONTINUE
      ELSEIF (NFLIP .EQ. 1 .AND. STORE(1) .LT. STORE(2)) THEN
        TEMP1 = THETA1
        TEMP2 = THETA2
        INDEX1 = I
        INDEX2 = J
        DO 60 M = 1, NBASIS + 1
          COEFF2(M) = COEFF(M)
60      CONTINUE
      ELSEIF (NFLIP .EQ. 1 .AND. STORE(2) .LT. STORE(1)) THEN
        STORE(1) = STORE(2)
      ELSE
        ENDIF
      STORE(NFLIP) = STORE(1)
    ENDIF
*      =====
*      Increment temperature for inner loop, and after last pass
*      print smallest SSE encountered in inner loop, then
*      increment temperature for outer loop.
*      =====

      THETA1 = THETA1 + DELTAT
70    CONTINUE
      PRINT*, STORE(1)
      THETA2 = THETA2 + DELTAT

```

80 CONTINUE

```
*      =====  
*      Print output.  
*      =====
```

PRINT*

PRINT*, 'I =', INDEX1, 'J =', INDEX2

PRINT*, 'THETA1 =', TEMP1, 'THETA2 =', TEMP2

PRINT*, 'Sum of the square of errors =', STORE(1)

PRINT*, 'Coefficients are: '

DO 90 M = 1, NBASIS + 1

PRINT*, COEFF2(M)

90 CONTINUE

END

```
*      =====  
*      Subroutine for basis functions.  
*  
*      Definitions:  
*      F      - Subroutine for computing values from user-  
*                supplied basis functions.  
*      K      - Basis function number.  
*      X      - X-axis value.  
*      THETA1 - Temperature for first basis function.  
*      THETA2 - Temperature for second basis function.
```

DOUBLE PRECISION FUNCTION F(K, X)

```

INTEGER K
DOUBLE PRECISION THETA1, THETA2, X
COMMON THETA1, THETA2
IF (K .EQ. 1) THEN
    F = X**3.0D+00 / (THETA1**4.0D+00 * (DEXP(X/THETA1)
$                                     - 1.0D+00))
ELSE
    F = X**3.0D+00 / (THETA2**4.0D+00 * (DEXP(X/THETA2)
$                                     - 1.0D+00))
ENDIF
RETURN
END

```

The following output is typical of the above program and was used to generate the two-Planckian fit in Figure 10 of Chapter V.

```
% f77 planck.f -limsl
```

```
planck.f:
```

```
  MAIN planck:
```

```
  f:
```

```
% a.out
```

```
  Number of points = 197
```

```
  Include intercept? (1 = Yes, 0 = No)
```

```
  0
```

```
  For investigation, start THETA1 and THETA2 at
```

```
  what temperatures (KeV)? (THETA1, THETA2)
```

```
  .409, .840
```

Increment temperatures by what DELTAT?

.001

Loop information. How many iterations for each
loop? (inside [THETA1], outside [THETA2])

3, 6

I = 1

3.0954533670417d-04

I = 2

3.0024962916826d-04

I = 3

2.9380294559385d-04

I = 4

2.9019676931351d-04

I = 5

2.8935158596325d-04

I = 6

2.8935158596325d-04

I = 5 J = 2

THETA1 = 0.41000000000000 THETA2 = 0.84400000000000

Sum of the square of errors = 2.8935158596325d-04

Coefficients are:

1.8698923739682d-02

0.13468654781493

0.

The two-Planckian fit is calculated from:

$$\alpha_0 = 0$$

$$\alpha_1 = 1.8698923739682E-02$$

$$\alpha_2 = 0.13468654781493$$

$$\theta_1 = 0.410$$

$$\theta_2 = 0.844$$

$$P_1 = E^3 / [\exp(E/\theta_1) - 1]$$

$$P_2 = E^3 / [\exp(E/\theta_2) - 1]$$

$$S_{\text{fit}}(E) = \alpha_0 + \alpha_1 \cdot P_1 + \alpha_2 \cdot P_2$$

Appendix C: Computer Programs to Calculate Binding
Energy and Temperature

The following computer program calculates the binding energy to remove the next bound electron from an atom and is written in Quick Basic (7).

```
' Maj Drew Fisher
' 5 Nov 89
' ZSTAR.BAS
' Ver. 1.0 5 Nov 89
' This program computes Zj* and Ej for use in Zstar.tk to
find free
' electrons vs temperature.

OPTION BASE 1
DEFINT I-N
SIZE = 10
REDIM xN(SIZE), SIGMA(SIZE, SIZE)

' = = = = =
' Slater screening constants from (3:169).
' Column 1 - 5.

DATA 0.6250, 0.9383, 0.9811, 0.987 , 0.994
DATA 0.2346, 0.6895, 0.8932, 0.94 , 0.97
DATA 0.1090, 0.3970, 0.7018, 0.85 , 0.92
DATA 0.0617, 0.2350, 0.4781, 0.705 , 0.83
DATA 0.0398, 0.1552, 0.3312, 0.531 , 0.72
DATA 0.0277, 0.1093, 0.2388, 0.400 , 0.854
```

DATA 0.0204, 0.0808, 0.1782, 0.3102, 0.459

DATA 0.0156, 0.0625, 0.1378, 0.2425, 0.371

DATA 0.0123, 0.0494, 0.1106, 0.1936, 0.299

DATA 0.0100, 0.0400, 0.0900, 0.1584, 0.245

' Column 6 - 10.

DATA 0.997 , 0.999 , 1.000 , 1.000 , 1.000

DATA 0.984 , 0.990 , 0.993 , 0.995 , 1.00

DATA 0.955 , 0.97 , 0.98 , 0.99 , 1.00

DATA 0.90 , 0.95 , 0.97 , 0.98 , 0.99

DATA 0.83 , 0.90 , 0.95 , 0.97 , 0.98

DATA 0.735 , 0.83 , 0.90 , 0.95 , 0.97

DATA 0.610 , 0.745 , 0.83 , 0.90 , 0.95

DATA 0.506 , 0.635 , 0.750 , 0.83 , 0.90

DATA 0.431 , 0.544 , 0.656 , 0.760 , 0.83

DATA 0.353 , 0.466 , 0.576 , 0.67 , 0.765

' = = = = =

' Read data into array SIGMA(I, J).

CLS

FOR I = 1 TO 10

FOR J = 1 TO 5

READ SIGMA(I, J)

NEXT J

NEXT I

FOR I = 1 TO 10

FOR J = 6 TO 10

```

        READ SIGMA(I, J)
    NEXT J
NEXT I
' = = = = =
' User input.
INPUT "Atomic number, Z"; Z
PRINT
INPUT "Level, J"; J
PRINT
INPUT "Number of free electrons per atom"; xNF
PRINT
INPUT "Number density [1/m^3]"; xNUMDEN
PRINT
' = = = = =
' Compute effective atomic number Zj*.
SUM1 = 0
FOR I = 1 TO J
    xN(I) = 2 * I ^ 2
    TEMP = SUM1
    SUM1 = SUM1 + xN(I)
    IF Z - xNF < SUM1 THEN xN(I) = Z - xNF - TEMP
NEXT I
SUM2 = 0
IF J > 1 THEN
    FOR I = 1 TO J - 1

```



```

        SUM2 = SUM2 + SIGMA(I, J) * xN(I)

    NEXT I

END IF

ZjSTAR = Z - SUM2 - xN(J) * (1 - 1 / (2 * J ^ 2)) * SIGMA(J,
J)

' = = = = =
' Compute ionization potential, Ej, to remove electron.
a0 = 5.292E-11 'Bohr radius [m].
eCHARGE = 1.602E-19 'Electron charge [C].
EPSILO = 8.854E-12 'Permittivity of vacuum [F/m]
PI = 3.14159
RYDBERG = 13.61 'Rydberg constant [eV].
rj2 = a0 ^ 2 * J ^ 4 / ZjSTAR ^ 2 * (7 / 4 + 5 / (4 * J ^
2))
R = (3 / (4 * PI * xNUMDEN)) ^ (1 / 3)
ENER = eCHARGE / (8 * PI * EPSILO * R) '[eV]
Ej = -RYDBERG * (ZjSTAR / J) ^ 2 + xNF * ENER * (18 / 5 -
rj2 / R ^ 2)

' = = = = =
' Print output.
PRINT "Atomic number = "; Z
PRINT "Number density [1/m^3] = "; xNUMDEN
PRINT "Level, J = "; J
PRINT "Electrons in J level (nj) = "; xN(J)
PRINT "Free electrons per atom (Z*) = "; xNF

```

```

PRINT "Effective atomic number (Zj*) = "; ZjSTAR
PRINT "Ionization potential (Ej) [eV] = "; Ej
PRINT
END

```

The next program computes the temperature corresponding to the binding energy calculated in the previous program.

===== VARIABLE SHEET ===== For Academic Use Only

St	Input	Name	Output	Unit	Comment
	5.685E-15	me		see >>	Electron mass in KeV(s/m)^2.
	4.136E-18	h		KeV-s	Planck constant.
	29	Z			Atomic number.
	-10868.9	Ej		eV	Ionization potential.
L	27.1	nf		1/atom	Free electrons per atom.
	1E27	Nv		1/m^3	Atomic number density.
	1	j			Principal quantum state.
	1.9	nj			Number of electrons in state j.
L		θ	.92942099	KeV	Temperature.
		P	.00038227		Parameter.

===== RULE SHEET ===== For Academic Use Only

S Rule

$$P = h^2 / (2 * \pi() * me) * (nf * Nv / 2 * (2 * j^2 / nj - 1))^{(2 / 3)}$$

$$\theta = -Ej / \ln((\theta / P)^{(1.5)})$$

Bibliography

1. Dolan, Thomas J. Fusion Research, Volume II - Experiments. New York: Pergamon Press, 1982.
2. Eisberg, Robert M. and Robert I. Resnick. Quantum Physics of Atoms, Molecules, Solids, Nuclei, and Particles (Second Edition). New York: John Wiley & Sons, Inc., 1985.
3. Pomraning, G. C. The Equations of Radiation Hydrodynamics. New York: Pergamon Press, 1973.
4. Bigelow, W. S. An "Onion" Ionization Model for Prediction of the Temperature Dependence of Ionization in Plutonium. Unpublished student paper for NENG 685. Air Force Institute of Technology (AU), Wright-Patterson AFB OH, undated.
5. Universal Technical Systems, Inc. TK Solver Plus software (Version 1.0 and 1.1). Rockford IL, 1987.
6. International Mathematical and Statistical Libraries, Inc. DFNSLQ FORTRAN subroutine (Version 1.0). Houston TX, April 1987.
7. Microsoft Corporation. Microsoft Quick Basic software (Version 4.5). Redmond WA, 1988.

Vita

Major Drew R. Fisher [REDACTED]

[REDACTED] He graduated from high school in Centerville, Ohio in 1974 and attended the United States Air Force Academy, from which he received the degree of Bachelor of Science in Physics in May 1978. Upon graduation, he entered the Air Force on active duty as a commissioned officer in May 1978 and completed navigator training, receiving his wings in March 1979. He served as a C-130 navigator and instructor navigator in the 21st Tactical Airlift Squadron (TAS), Clark AB, Philippines from July 1979 to July 1982. From October 1982 to October 1985 he served as an instructor and flight evaluator navigator flying C-130s with the 37 TAS, out of Rhein Main AB, West Germany. He then taught at the C-130 Tactical Airlift Instructor School as an instructor and flight evaluator navigator with the 34th Technical Training Squadron, until entering the School of Engineering, Air Force Institute of Technology, in June 1988.

[REDACTED]

[REDACTED]

REPORT DOCUMENTATION PAGE				Form Approved OMB No. 0704-0188	
1a. REPORT SECURITY CLASSIFICATION UNCLASSIFIED			1b. RESTRICTIVE MARKINGS		
2a. SECURITY CLASSIFICATION AUTHORITY			3. DISTRIBUTION/AVAILABILITY OF REPORT Approved for public release; distribution unlimited		
2b. DECLASSIFICATION/DOWNGRADING SCHEDULE					
4. PERFORMING ORGANIZATION REPORT NUMBER(S) AFIT/GNE/ENP/90M-1			5. MONITORING ORGANIZATION REPORT NUMBER(S)		
6a. NAME OF PERFORMING ORGANIZATION School of Engineering		6b. OFFICE SYMBOL (If applicable) AFIT/ENP	7a. NAME OF MONITORING ORGANIZATION		
6c. ADDRESS (City, State, and ZIP Code) Air Force Institute of Technology (AU) Wright-Patterson AFB, Ohio 45433-6583			7b. ADDRESS (City, State, and ZIP Code)		
8a. NAME OF FUNDING/SPONSORING ORGANIZATION		8b. OFFICE SYMBOL (If applicable)	9. PROCUREMENT INSTRUMENT IDENTIFICATION NUMBER		
8c. ADDRESS (City, State, and ZIP Code)			10. SOURCE OF FUNDING NUMBERS		
			PROGRAM ELEMENT NO.	PROJECT NO.	TASK NO.
			WORK UNIT ACCESSION NO.		
11. TITLE (Include Security Classification) TIME-INTEGRATED SPECTRUM OF A RADIATIVELY COOLING PLANCKIAN EMITTER					
12. PERSONAL AUTHOR(S) Drew R. Fisher, MAJ, USAF					
13a. TYPE OF REPORT MS Thesis		13b. TIME COVERED FROM _____ TO _____		14. DATE OF REPORT (Year, Month, Day) 1990 March	
15. PAGE COUNT 100					
16. SUPPLEMENTARY NOTATION					
17. COSATI CODES			18. SUBJECT TERMS (Continue on reverse if necessary and identify by block number) Spectral energy distribution, Planckian, Heat capacity, Energy levels		
FIELD	GROUP	SUB-GROUP			
20	05				
19. ABSTRACT (Continue on reverse if necessary and identify by block number) Thesis Advisor: Kirk A. Mathews, LCDR, USN Assistant Professor of Nuclear Engineering <div style="text-align: center; margin-top: 20px;">(over)</div>					
20. DISTRIBUTION/AVAILABILITY OF ABSTRACT <input checked="" type="checkbox"/> UNCLASSIFIED/UNLIMITED <input type="checkbox"/> SAME AS RPT. <input type="checkbox"/> DTIC USERS			21. ABSTRACT SECURITY CLASSIFICATION UNCLASSIFIED		
22a. NAME OF RESPONSIBLE INDIVIDUAL Kirk A. Mathews, LCDR, USN			22b. TELEPHONE (Include Area Code) (513) 255-4498		22c. OFFICE SYMBOL AFIT/ENP

UNCLASSIFIED

This paper investigates the effect of cooling a hot Planckian emitter upon its fluence spectrum . A sequence of models of increasing complexity is developed to determine the effects of various aspects of cooling upon the spectrum, such as initial temperature, density, and ionization state of the plasma. Spectra are calculated for radiating plasmas composed of different atomic number materials (carbon, aluminum, copper, and plutonium) at initial temperatures of 0.02 - 10 KeV, and initial densities of $1E+25$ - $1E+29$ atoms/m³, to observe the effects of these parameters on the fluence spectrum. The change in material and binding energy for some spectra at the low energy end produces a second, prominent but smaller peak. The resulting non-Planckian spectra can be approximated with two or more Planckian basis functions having different temperatures. *Tueses. (j20)*

UNCLASSIFIED